# Bay of Plenty
# Primary Production Modelling: Aquaculture Management Areas

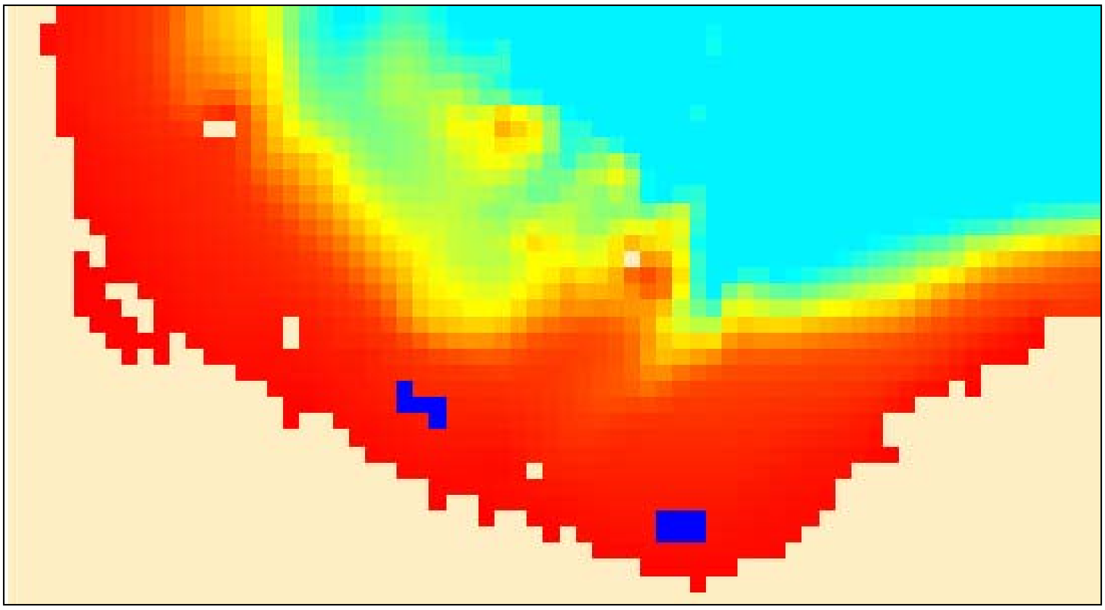

**For**

Environment Bay of Plenty
REGIONAL COUNCIL

Environment Bay of Plenty

Marine Consulting and Research

**September 2006**

# Bay of Plenty
# Primary Production Modelling: Aquaculture Management Areas

## Report Status

| Version | Date | Status | Approved By: |
|---|---|---|---|
| V.1 | May 2006 | Draft | KPB |
| V.2 | July 2006 | Rev. A | STM |
| V.3 | September 2006 | Final | KPB |

It is the responsibility of the reader to verify the currency of the version number of this report. All subsequent releases will be made directly to the Client.



**Acknowledgements**

This work was conducted for Environment Bay of Plenty. EBOP staff participated in the collection of data. We particularly thank the EBOP Project Leader Stephen Park for his very helpful involvement and Shane Iremonger for his assistance with provision of data and field work. Others closely involved were Paul Dell and Aileen Lawrie. The co-operation of the University of Waikato Coastal Marine Group is also warmly acknowledged.

# Bay of Plenty
# Primary Production Modelling : Aquaculture Management Areas

# Primary Production Modelling, and Assessment of Large Scale Impacts of Aquaculture Management Areas on the Productivity within the Bay of Plenty.

Peter Longdill[1, 2]
Kerry Black[1]
Tim Haggitt[3]
Shaw Mead[1]

[1] ASR LTD, Marine Consulting and Research, 1 Wainui Rd, Raglan, New Zealand +64 7 8250380.
[2] Coastal Marine Group, University of Waikato, Private Bag 3105, Hamilton, New Zealand.
[3.] Coastal and Aquatic Systems, PO Box 54, Leigh, New Zealand

**Report prepared for Bay of Plenty Regional Council**

## EXECUTIVE SUMMARY

The potential effects of several large aquaculture (mussel) farms within the Bay of Plenty have been simulated with a calibrated ecological model. The depletion of phytoplankton and zooplankton are determined for scenarios of two and four large mussel farms (approximately 5000 Ha each) with different relative positions on the inner shelf of the central Bay of Plenty.

When averaged over a year, the proposed farms (Opotiki and Pukehina) reduce the phytoplankton in a region some 40 km by 20 km by approximately 1% in the surface waters of the Bay (0-5 m depth). This depletion represents a decrease of ~ 0.04 $mg/m^3$ chlorophyll-*a* from a typical average value of ~ 4.5 $mg/m^3$. The mussel farms increase the local ammonia concentration by approximately 0.001 $g/m^3$, and deplete the local dissolved oxygen concentration by approximately 0.002 $g/m^3$, from background values of typically 0.05 $g/m^3$ and 8 $g/m^3$ respectively.

More severe impacts are evident at the depth layer in the water column where the mussels are located (15-25 m), with phytoplankton abundance reductions of 4-8% being predicted when averaged over the full year. The higher impacts at depth occur over a region some 12 x 6 km, i.e. they are mostly restricted to the environs of the farm and the adjacent coast. Of course, the zone where phytoplankton abundance is reduced is proportional to the total area and mussel density of the farms.

To specify carrying capacity of the Bay, the issue to address is whether these reductions to phytoplankton and zooplankton are biologically significant. In particular, while the abundances may be reduced by 4-8% when averaged over the year, the percentage reductions are higher in seasons when natural phytoplankton abundance is lower. Thus, there are both annual and seasonal effects, which will potentially impact on the broader eco-system, which is equally subject to seasonal dynamics.

It is unlikely that the production carrying capacity of the Bay of Plenty system will be adversely affected by the level of aquaculture modelled in this study, as even maximum depletion rates resulted in chlorophyll-*a* levels well above published

threshold production carrying capacity levels identified for mussel farming in other parts of New Zealand, e.g., ~ 1 µg $L^{-1}$. Given the physical and biological characteristics of the Bay of Plenty area, relative to the predicted levels of impact presented here, it is also unlikely that the ecosystem carrying capacity will be adversely affected. Further model simulations are currently underway to consider the influence of climatic factors such as El Nino/La Nina events.

Further assessments of the ecosystem carrying capacity can be achieved by additional modelling and investigating present knowledge gaps, particularly the variation in phytoplankton species composition through space and time within the Bay of Plenty and impacts on the zooplankton community. Other factors that also impact on ecosystem health and warrant investigation are the significance of zooplankton mortality due to marine farms with respect to recruitment of other water-borne marine organisms and the potential impacts of mussel spat colonisation to new locations outside the marine farms (resulting to a decreased of marine biodiversity and/or community change).

# TABLE OF CONTENTS

## LIST OF FIGURES

## LIST OF TABLES

# INTRODUCTION

## *1.1 BACKGROUND – THE PROJECT*

New Zealand has been experiencing a rapid growth in the aquaculture industry in recent years. This growth, coupled with outdated legislation has prompted the government to reform the aquaculture legislation. The reforms took effect on 1 January 2005, amending five different Acts:

- Resource Management Amendment Act (No 2) 2004
- Fisheries Amendment Act (No 3) 2004
- Conservation Amendment Act 2004
- Biosecurity Amendment Act 2004
- Te Ture Whenua Maori Amendment Act (No 3) 2004

It also created two new Acts:

- Maori Commercial Aquaculture Claims Settlement Act 2004
- Aquaculture Reform (Repeals and Transitional Provisions) Act 2004

Under the new laws, new marine farms can now only be established within zones called Aquaculture Management Areas (AMAs). An AMA must be a defined area, mapped and described in the regional coastal plan. In considering AMAs, councils must consider the effects of aquaculture on the environment, fisheries resources, fishing interests and other uses of the coastal marine area. One of the central considerations in establishing AMA's is sustainability of the natural resources. This creates a need for a scientifically defendable understanding of the physical interactions in the offshore environment and the likely effects of any proposal.

Recent advances in technology coupled with pressure for space within the coast has seen proposals for large offshore farms. A single mussel farm of 4,750 ha has interim approval (Mfish Interim decision 2006) offshore from Opotiki (Figure 1.1). A further pre-moratorium mussel farm application for 3,800 ha near Pukehina/Otamarakau, in the central Bay of Plenty is yet to be heard (Figure 1.1). While there are many uncertainties with the expansion of aquaculture in the Bay of Plenty, there are many opportunities for both filter feeders and other species. As the Regional Council are in the "driving" seat for planning for aquaculture, a robust and defensible understanding of the offshore Bay of Plenty is needed. This work provides a basis for decisions for the understanding of how marine farming is likely to affect the physical dynamics and biological values of the Bay of Plenty.

If aquaculture is to be advanced in the Bay of Plenty the council needs to:

- Ensure the current proposals are monitored and are sustainable; and
- Make decisions about other sites suitable for aquaculture, which sustain the environment and lead to an effective aquaculture industry.

Mussels and other filter feeders are known to extract both phytoplankton and zooplankton from the water column. Moreover, most nutrients arriving at the coast come from deeper water in the bottom mixed layer (Park, 1998) (Fig. 1.1). To reach the coast, this nutrient-rich seawater must pass through the AMAs and so impacts on the inshore wider environment need to be understood.

The goals of this project were to provide focused information over-viewing the Bay of Plenty for planning of AMAs. The aims were achieved by establishing data collection programmes coupled with sophisticated numerical models. Thus, any scenario can be modelled to provide information on the likely effects.

Regional councils are also obliged to monitor cumulative effects of activities. This work also can be readily absorbed into the regional monitoring programs or for particular farms.

This information provides significant potential benefits to the aquaculture industry by providing background information on the nature of the offshore environment and providing the tools by which effects of any proposal can be assessed.

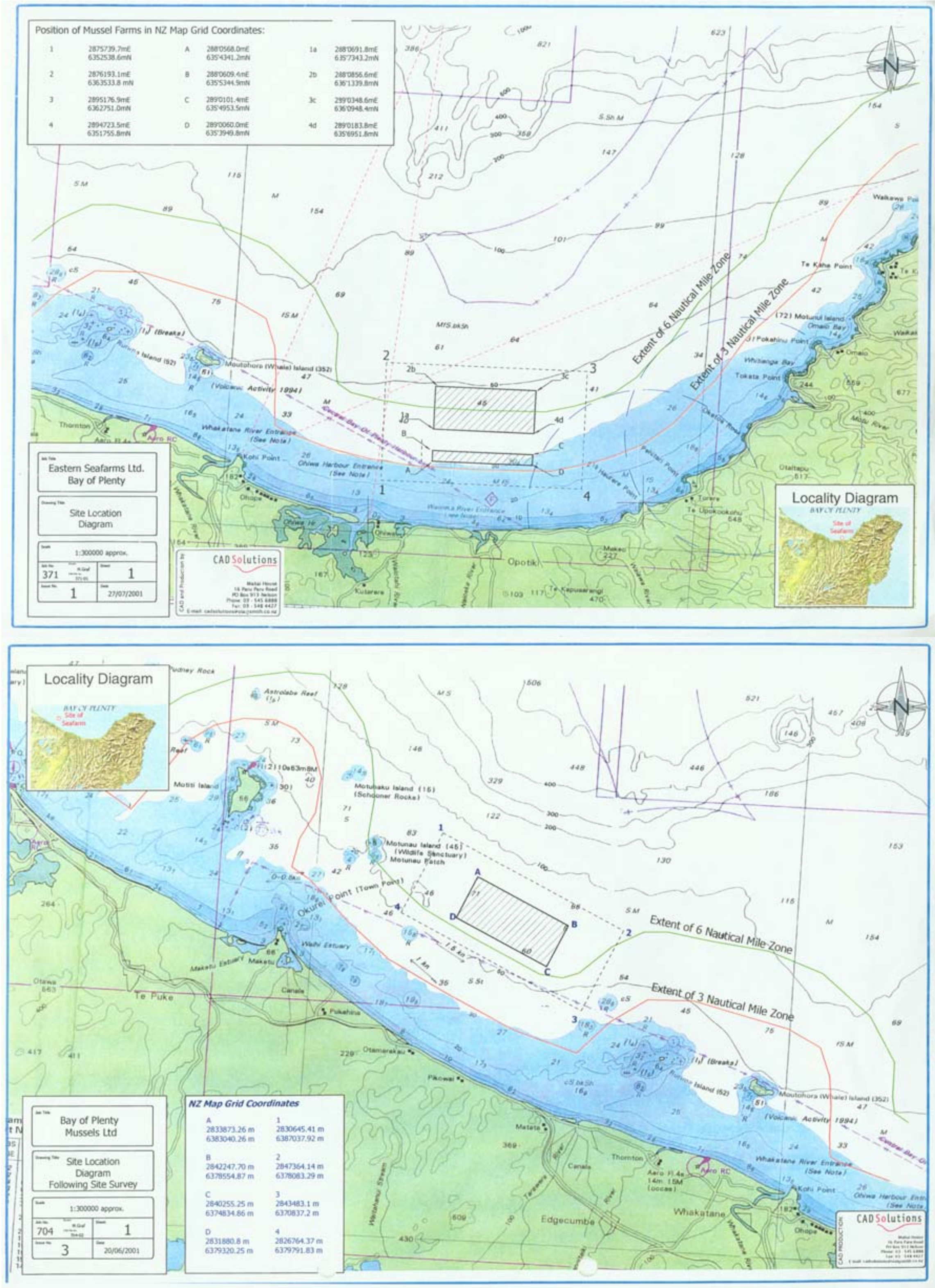


**Figure 1.1** – Proposed offshore aquaculture sites in the Bay of Plenty

### *1.1.1 STUDIES UNDERTAKEN*

To redress the lack for data and understanding of the system, EBoP commissioned ASR Ltd as follows:

- To be informed about offshore oceanographic and ecological systems when choosing open coast AMA sites, for a sustainable environment, kaimoana and aquaculture industry in the Bay of Plenty

The goals were achieved by:

- Establishing monitoring stations and undertaking regular surveys of water properties, currents and waves
- Undertaking numerical modelling of circulation and physical dynamics
- Undertaking numerical modelling of the food chain (food dynamics modelling), with particular focus on green mussels
- Developing recommendations about the carrying capacity of sites around the Bay of Plenty

The present report deals with the numerical modelling of primary production and the impacts of large scale green-lipped mussel farming within the Bay of Plenty. While AMA designation within the Bay of Plenty system could be used for a variety of different aquaculture types e.g., sponge, scallop, fin-fish and mussel aquaculture, this study has used mussel aquaculture to examine likely effects on primary production and carrying capacity. This is predominantly due to large mussel farms representing the present applications, and the fact that mussel culture has received the most attention with respect to effects on primary production and carrying capacity and as such, useful benchmarks using chlorophyll *a* levels have been derived for determining likely impacts and effects (e.g., Inglis *et al.* 2005). Mussels feed on phytoplankton, zooplankton, detritus and other organic particles in the size-range 3-200 µm. which they filter from the water column, and large mussels can filter up to 350 liters of water per day.

### *1.2 BACKGROUND-REPORT STRUCTURE*

This report describes sophisticated numerical modelling of the primary production and water column ecology within the Bay of Plenty. Model methodology and its application to the study site are covered and modelling results are compared with measured data from several field data collection surveys. The list of reports that are relevant to the study are listed below:

- Black, K.P., Beamsley, B., Longdill, P., Moores, A., 2005 *Current and Temperature Measurements: Aquaculture Management Area.* Report prepared by ASR Consultants for Bay of Plenty Regional Council, March 2005.

- Longdill, P.C., Black, K.P., Park, S. and Healy, T.R., 2005. *Bay of Plenty Shelf Physical and Chemical Properties 2003-2004 : Choosing open coast AMAs to sustain the environment, kaimoana and aquaculture industry.* Report for Environment Bay of Plenty, ASR Ltd, P.O. Box 67, Raglan, NZ, and the University of Waikato. 35p

- Longdill, P. C., and Black, K. P., and Healy, T.R. 2005. *Locating aquaculture management areas – an integrated approach.* Report for Environment Bay of Plenty, ASR Ltd, P.O. Box 67, Raglan, NZ, and the University of Waikato. 53p.

- Longdill, P.C., Black, K.P. 2006. *Numerical Hydrodynamic Modelling: Aquaculture Management Areas.* Report for Environment Bay of Plenty, ASR Ltd, PO Box 67, Raglan, New Zealand. 67p.

- Longdill, P.C., Black, K.P., Haggit, T. and Mead, S.T., 2006. *Primary Production Modelling, and Assessment of Large Scale Impacts of Aquaculture Management Areas on the Productivity within the Bay of Plenty.* Report for Environment Bay of Plenty, ASR Ltd, PO Box 67, Raglan, New Zealand. 51p

- Mead, S.T., Longdill, P.C., Moores, A., Beamsley, B., and Black, K.P. 2005. *Underwater Video, Grab Samples and Dredge Tows of the Bay of Plenty Sub-Tidal Area (10- 100 m depth).* Report for Environment Bay of Plenty, ASR Ltd, PO Box 67, Raglan, New Zealand. 34p

- Park, S.G. and Longdill, P.C. 2006. Synopsis of SST and Chl-a in Bay of Plenty waters by remote sensing. *Environment BOP Environmental Publication 2006/13. Environment Bay of Plenty, PO Box 364, Whakatane*.

Various aquaculture scenarios are simulated with the model which provides valuable insights into potential impacts and spatial extents of influences from large-scale offshore aquaculture within the Bay of Plenty.

The structure of the report is as follows:

**Section 1** Introduction and background to the project.

**Section 2** Model background – 3DDLIFE.

**Section 3** Model runs and calibration.

**Section 4** Mussel farming aquaculture scenarios

**Section 5** Summary of results.

# 2 MODEL BACKGROUND

## *2.1 3DDLIFE – MODEL FORMULATION*

### *2.1.1 BACKGROUND*

The model 3DDLIFE is a Eulerian based, fixed stoichiometry coastal marine ecosystem productivity model. The model solves multiple interactive equations for the state variables in a forward explicit time-stepping scheme, with the variables represented on a regular grid. The model describes nutrient cycling (nitrogen and phosphorus), phytoplankton and zooplankton growth and decay along with the dissolved oxygen conditions within the coastal marine environment, though its primary concern is phytoplankton and zooplankton dynamics.

The model 3DDLIFE is coupled to the 3DD hydrodynamic model from the commercial 3DD Suite (© Black, 2001) in order to simulate the concurrent processes of advection, dispersion, ecology and biology. Information from the hydrodynamic model used by 3DDLIFE includes the 3-dimensional water velocities to determine the advection and dispersion of variables, while the water temperature and salinities are used to determine reaction rates which are sensitive to these parameters. Details relating to the hydrodynamic model methods, calibration and validation are included in an accompanying report (Longdill and Black, 2006).

Required inputs for 3DDLife include solar radiation and wind velocities at 10 m above Mean Sea Level (MSL), along with boundary conditions at all open boundaries within the grid detailing the concentration of all 8 state variables throughout the simulation (Table 2.1).

**Table 2.1** State variables, abbreviations and units used in 3DDLIFE.

| State Variable | Abreviation | Units |
|---|---|---|
| Phytoplankton (dry weight biomass) | P | $g/m^3$ |
| Zooplankton (dry weight biomass) | Z | $g/m^3$ |
| Nitrate + Nitrite | NOx | $g/m^3$ |
| Ammonia | NH3 | $g/m^3$ |
| Detrital Nitrogen | DN | $g/m^3$ |
| Inorganic Phosphorus | PO4 | $g/m^3$ |
| Detrital Phosphorus | DP | $g/m^3$ |
| Dissolved Oxygen | DO | $g/m^3$ |

The processes simulated by the model include (Figure 2.1):

- phytoplankton production,
- phytoplankton sedimentation,
- non-predatory phytoplankton death,
- grazing by zooplankton,
- zooplankton excretion,
- zooplankton respiration,
- non-predatory zooplankton death,
- mineralization of suspended detritus,
- sedimentation of detritus,
- mineralization of detritus on the bed,
- nitrification of ammonia, and
- re-aeration at the air-water interface
- green-lipped mussel grazing

Details of these various functions within 3DDLIFE are presented in Appendix 1.

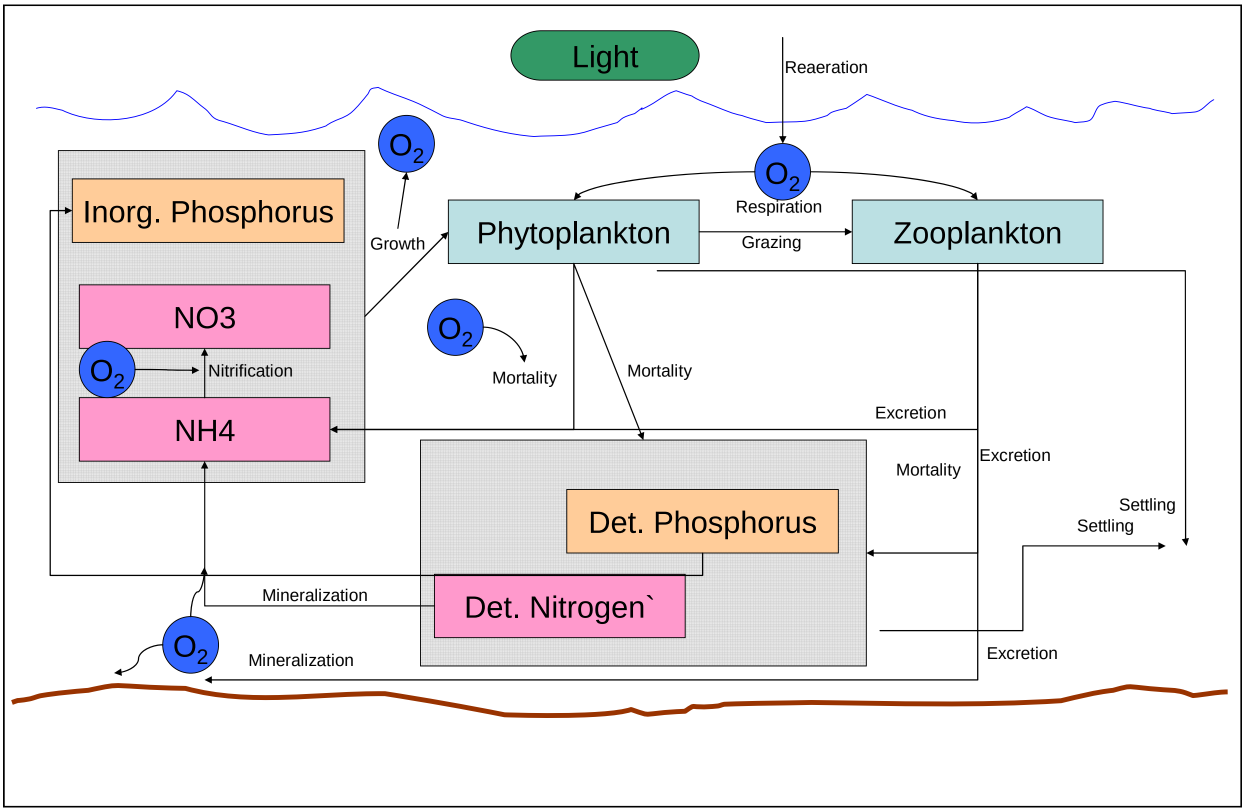


**Figure 2.1 –** Simplified flow diagram of fluxes of nitrogen and phosphorus within the model 3DDLIFE.

### *2.2 CALIBRATION*

The model 3DDLIFE was calibrated at several sites within the Bay of Plenty based on field measurements detailed in Longdill *et al.* (2005) and Park *et al.* (2006). A summary of the model parameters, constants and coefficients are detailed in Table 2.2

**Table 2.2 –** Model parameters used in the Bay of Plenty**.**

| **Name** | **Value** | **Units** | **Source** |
|---|---|---|---|
| Time step | 0.01 | Days | N/A |
| | | | |
| Phytoplankton phosphorus ratio | 0.02 | N/A | Redfield ratio weights |
| Phytoplankton nitrogen ratio | 0.14 | N/A | Redfield ratio weights |
| Optimal light intensity for photosynthesis | 70 | | |
| Phytoplankton (total) maximal growth rate | 1.2 | $day^{-1}$ | Thomann and |

| | | | |
|---|---|---|---|
| (20C) | | | Fitzpatrick (1982) Numerous references in Bowie et al. (1985) |
| Nitrogen half saturation constant for growth (phyto) | 0.025 | $g/m^{-3}$ | Numerous references in Bowie et al. (1985) |
| Phosphorus half saturation constant for growth (phyto) | 0.001 | $g/m^{-3}$ | Numerous references in Bowie et al. (1985) |
| Phytoplankton maximal non-predatory mortality (20C) | 0.7 | $day^{-1}$ | Calibrated |
| Reference settling velocity of phytoplankton | 0.1 | $m.day^{-1}$ | Numerous references in Bowie et al. (1985) |
| Fraction of dead phytoplankton undergoing immediate mineralization | 0.15 | N/A | Calibrated |
| Phytoplankton temperature adjustment coefficient | 1.066 | N/A | Eppley (1972) |
| Phytoplankton non-predatory mortality temperature adjustment coefficient | 1.3 | N/A | Calibrated |
| | | | |
| Zooplankton assimilation efficiency | 0.4 | N/A | Calibrated |
| Half saturation constant for zooplankton feeding and growth | 0.05 | $gDWalgae.m^{3}$ | Calibrated |
| Zooplankton respiration rate at 20$^{o}$C | 0.05 | $day^{-1}$ | Numerous references in Bowie et al. (1985) |
| Zooplankton mortality rate at 20$^{o}$C | 0.05 | $day^{-1}$ | Numerous references in Bowie et al. (1985) |
| Fraction of zooplankton excreted material immediately mineralised | 0.4 | N/A | Calibrated |
| Oxygen conc. indicating depressed | 7 | $g/m^{-3}$ | DHI (2000) |
| zooplankton temperature adjustment function | 1.066 | N/A | |
| Threshold phytoplankton concentration below which feeding does not occur | 0.1 | $g/m^{-3}$ | Calibrated |
| | | | |
| Mineralisation rate of detrital nitrogen to NH3 | 0.005 | $day^{-1}$ | Calibrated |
| Temperature coefficient for mineralization of detrital nitrogen to NH3 | 1.01 | N/A | |
| Nitrification rate of NH3 to NOx | 0.027 | $day^{-1}$ | Calibrated |
| Temperature coefficient for nitrification | 1.06 | N/A | |
| | | | |
| Mineralisation rate of detrital phosphorus to PO4 | 0.03 | $day^{-1}$ | Calibrated |
| Temperature coefficient for mineralization of detrital phosphorus to PO4 | 1.066 | N/A | |
| | | | |
| Detritus sedimentation velocity | 5 | $m.day^{-1}$ | Calibrated |
| | | | |
| Albedo | 0.08 | N/A | |
| Long wavelength decay constant | 0.5 | N/A | Calibrated |
| Short wavelength decay constant | 0.0352 | N/A | Calibrated |
| | | | |

The model was run for an entire year, with an initial start date of 1 August 2003 which was chosen to match the periods of field data collection and because the water column was free of thermal stratification which makes the initial conditions in the model more easily defined and accurate. Input solar radiation was taken from Tauranga airport, wind velocities from Quikscat satellite scatterometer data, and riverine nutrient inputs assessed from typical concentrations detailed in Taylor and Park (2001). Current patterns came from a 1-year hydrodynamic simulation with Model 3DD. The model has 10 vertical layers and a 3000 x 3000 m horizontal grid size. Vertical layer thicknesses were 5, 10, 10, 10, 15, 20, 80, 100, 250, 500 m respectively from the sea surface to the seabed.

Figures 2.4 to 2.6 show calibration time series plots of modelled and sampled phytoplankton chlorophyll within the Bay of Plenty. These results are the outcome of sensitivity testing that led to the selection of coefficients in Table 2.2. The model has reproduced the variations in phytoplankton, both in time and through the water column. Other variables in the model (not shown here) also calibrate well. Given the complexity of the hydrodynamic and primary production models, which require a broad range of inputs and empirical coefficients, the results are satisfactory. Confidence in the results was greatly improved by the comprehensive use of a range of data (e.g. field measurements, satellite data, etc.) for calibration of the hydrodynamic model (presented in Longdill and Black, 2006), the large number of coefficients that have been previously used and presented in existing relevant literature (i.e. the source of 40% of the parameters listed in Table 2.2), and also because other coefficients that were used for calibration were not changed greatly from their base levels.

While there are some deviations in phytoplankton predictions, it is noted that the measured data is not fully consistent. The 3 field measurements were (1) CTD fluorometer measurements over appropriate depths, (2) chlorophyll-*a* from water samples, and (3) scufa fluorometer readings from water samples at discrete depths within that model layer. Notably the three different measurements are not always compatible and the scatter in the field data is similar to the scatter between the model and the measurements. The model prediction is mostly (not always) within the range of the 3 sets of measurements and so little improvement to the model may be achieved without further field data.

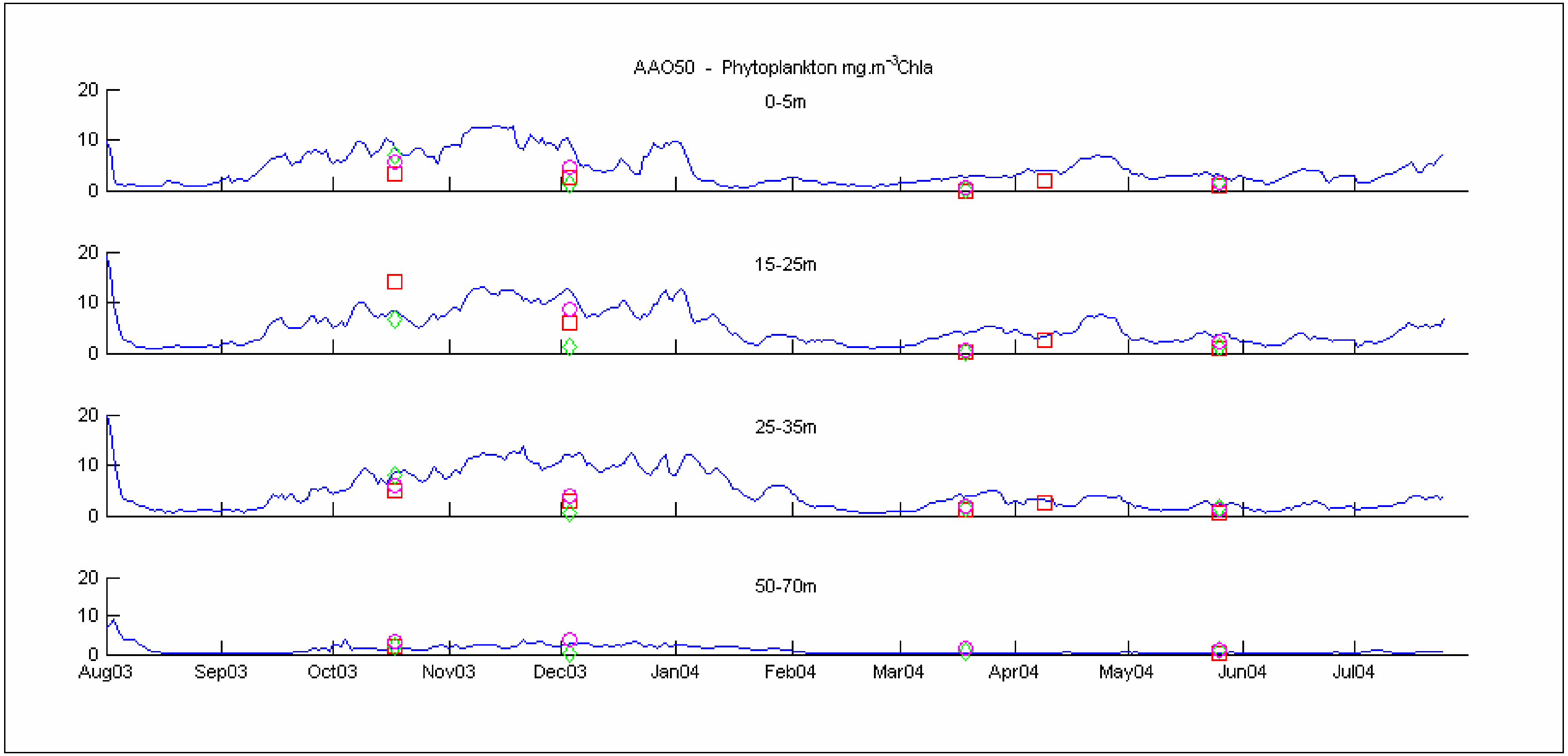


**Figure 2.2 –** Modelled (blue line) and measured phytoplankton chlorophyll-a between August 2003 and July 2004 at the Opotiki 50 m site. Red squares are averages of CTD fluorometer measurements over appropriate depths, green diamonds are chlorophyll-a from water samples, and pink circles are scufa fluorometer readings from water samples at discrete depths within that model layer.

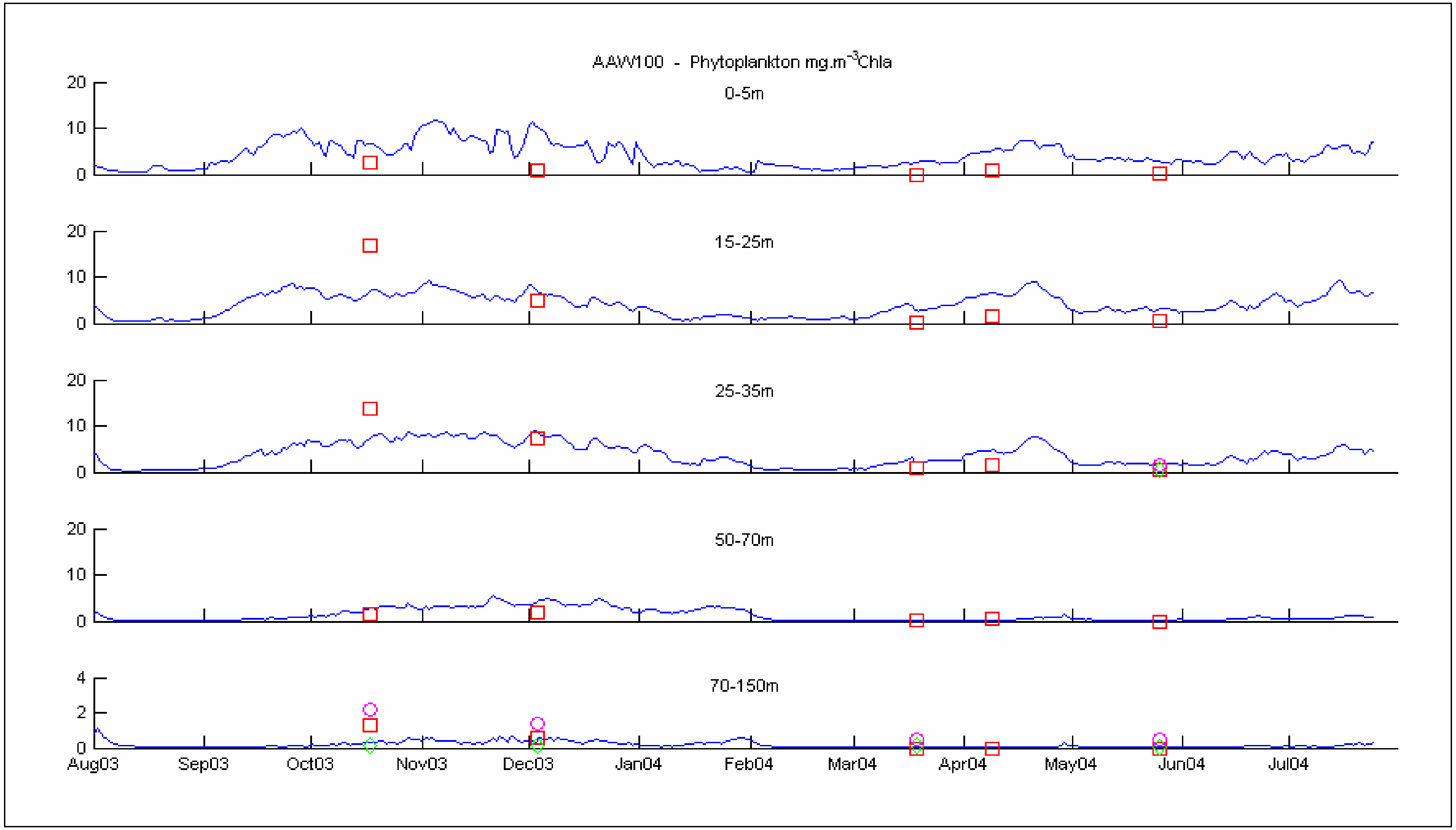


**Figure 2.3 –** Modelled (blue line) and measured phytoplankton chlorophyll-a between August 2003 and July 2004 at the Whakatane 100 m site. Red squares are averages of CTD fluorometer measurements over appropriate depths, green diamonds are chlorophyll-a from water samples, and pink circles are scufa fluorometer readings from water samples at discrete depths within that model layer.

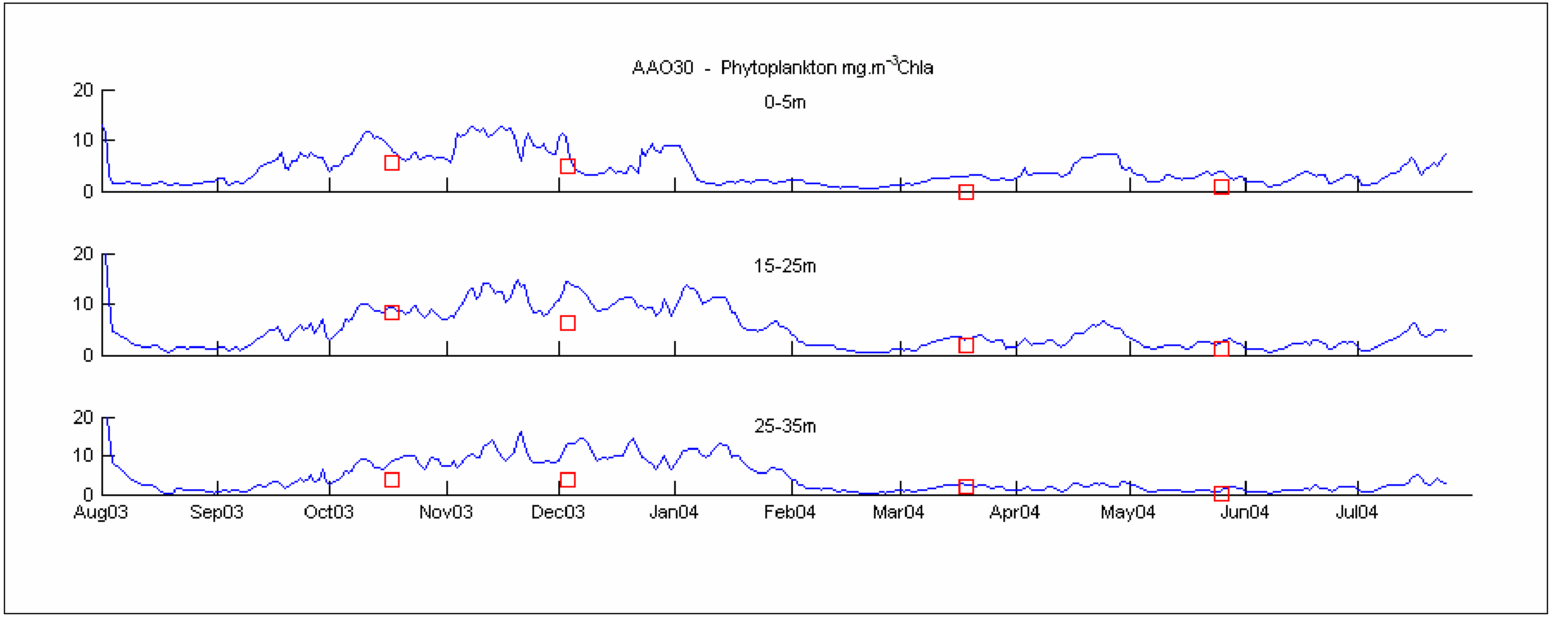


**Figure 2.4 –** Modelled (blue line) and measured phytoplankton chlorophyll-a between August 2003 and July 2004 at the Opotiki 30 m site. Red squares are averages of CTD fluorometer measurements over appropriate depths.

# 3 YEARLY-AVERAGED PHYTOPLANKTON ABUNDANCES

Several outputs can be taken from the simulations, including averages. The cholorophyll-*a* averaged over the year in the surface layer (0-5 m) is shown in Figure 3.1 and there are some large spatial variations in the levels. Typically phytoplankton concentrations are predicted to be greater near the coast. The nutrients used by the phytoplankton are provided by both the river inputs and nutrient-rich deep water upwelling to the coast. The circulation creates a tongue of phytoplankton that extends along East Cape. Highest levels are predicted to be on the shelf, near the coast in the Central Bay of Plenty, off the Pukehina/Otarmarakau/Matata area. There is a reduction in levels to the east of Opotiki at the base of East Cape.

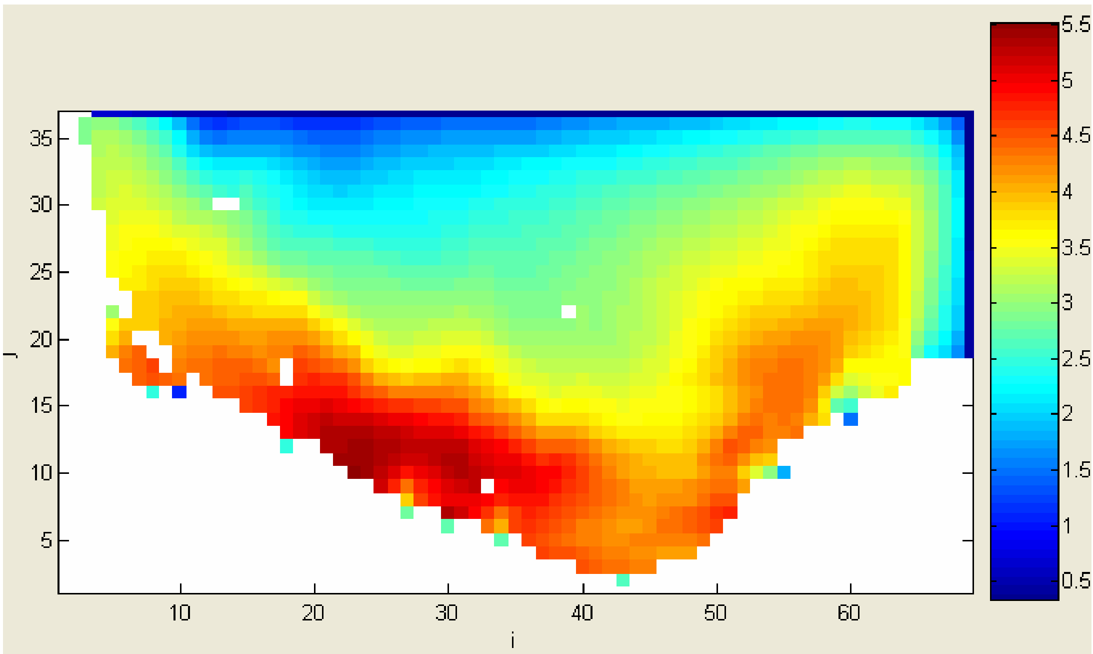


**Figure 3.1** – Modelled yearly averaged phytoplankton chlorophyll-*a* (mg/m3) in the surface layer within the Bay of Plenty.

## *3.1 AQUACULTURE SCENARIOS*

Various aquaculture scenarios have been modelled and the differences between the 'no-aquaculture model runs' and the 'with aquaculture model runs' calculated.

To calculate stocking density of the green-lipped mussels the following assumptions have been made:

- That the mussels are to be grown between 15 and 25 m of water
- That backbone length is 200 m and this carries 3100 m of dropper rope with a density of 180 mussels per meter of dropper

The actual farm mussel carrying capacity (used for modelling) is based on general industry operations practise, which was identified in a number of existing reports, and incorporates the planned stocking levels for the marine farms proposed for the Bay of Plenty. This resulted in the following classes of mussel stocking:

- 5% of the lines empty
- 10% used for spat catching
- 28.3% carry 35mm mussels
- 28.3% carry 75mm mussels
- 28.3% carry 95mm mussels

Based on these densities and using formulae published in James *et al.* (2001) and Marsden and Weatherhead (1999) mussel dry weight densities, clearance rates, excretion rates and respiration rates were calculated. Three different farm scenarios are considered:

- Two farms at Opotiki and Pukehina (similar to the proposed farms)
- Four farms spread along the coast
- Four farms placed on a cross-shore transect

Chlorophyll *a* within the Bay of Plenty is spatially and temporally variable being highest in coastal waters between August and January (Austral spring-summer) at all depths examined. Overall results are presented in Table 3.1. Chlorophyll *a* was typically higher in the Pukehina region than Opotiki. (refer to Tab. 3.1). The CD-ROM attached to this report presents yearly and seasonal results (both concentration and percentage difference of Chlorophyll-*a*) for the 3 different mussel farm scenarios (presented below) in the surface, 15 m deep and 25 m deep layers.

**Table 3.1 –** Results from modelling scenarios for three depth ranges examined for each farm scenario. Farm scenario 1 – Two farms at Opotiki and Pukehina; Farm scenario 2 – Four farms long-shore; Farm scenario 3 – Four farms cross-shore. Table denotes ambient seasonal range of chlorophyll *a* ($\mu L^{-1}$) and corresponding percent decrease relative to each farming scenario for each time period . Yearly averages are also presented.

| Farm Scenario 1 | Time | Pukehina | | Opotiki | |
|---|---|---|---|---|---|
| | | Range $\mu L^{-1}$ | % decrease | Range $\mu L^{-1}$ | % decrease |
| Surface waters | Aug-Oct | 4.5-7.0 | 0.2-0.45 | 4.5-6.0 | 0.3-0.6 |
| | Nov-Jan | 5.5-8.25 | 0.2-0.6 | 5.5-6.5 | 0.1-0.6 |
| | Feb-Apr | 2.5-3.25 | 1.0-2.25 | 2.5-3.25 | 1.5-2.5 |
| | May-Jul | 2.5-4.5 | 0.6-1.2 | 2.5-3.5 | 0.8-1.2 |
| | Yearly Average | | 0.4-1.0 | | 0.6-1.2 |
| | | Range $\mu L^{-1}$ | % decrease | Range $\mu L^{-1}$ | % decrease |
| 15 m | Aug-Oct | 3.5-7.0 | 0.2-0.55 | 4.0-6.0 | 0.45-0.8 |
| | Nov-Jan | 4.0-8.0 | 0-0.8 | 4.0-8.0 | 0-3.0 |
| | Feb-Apr | 2.75-3.5 | 0.5-2.0 | 2.75-3.75 | 0-3.0 |
| | May-Jul | 3..0-5.0 | 0.5-1.6 | 0-4.75 | 1.0-1.6 |
| | Yearly Average | | 0.6-1.4 | | 0.4-1.5 |
| | | Range $\mu L^{-1}$ | % decrease | Range $\mu L^{-1}$ | % decrease |
| 25m | Aug-Oct | 3.0-6.0 | 0.5-4.5 | 4.0-5.5 | 0.5-4.5 |
| | Nov-Jan | 2.5-7.0 | 0-7.0 | 4.0-9.5 | 0-7.0 |
| | Feb-Apr | 2.25-3.75 | 1.5-6.0 | 2.5-3.75 | 0-9.0 |
| | May-Jul | 2.5-4.5 | 1.0-5.5 | 2.5-4.0 | 1.0-5.5 |
| | Yearly Average | | 0-2.25 | | 0-3.5.0 |

| Farm Scenario 2 | Time | Pukehina | | Opotiki | |
|---|---|---|---|---|---|
| | Period | Range $\mu L^{-1}$ | % decrease | Range $\mu L^{-1}$ | % decrease |
| Surface waters | Aug-Oct | 4.5-7.0 | 0.4-1.0 | 4.5-6.0 | 0.6-1.0 |
| | Nov-Jan | 5.5-8.25 | 0.4-1.4 | 5.5-6.5 | 0.2-1.4 |
| | Feb-Apr | 2.5-3.25 | 2.25-4.0 | 2.5-3.25 | 3.0-4.5 |
| | May-Jul | 2.5-4.5 | 1.5-2.5 | 2.5-3.5 | 1.75-2.5 |
| | Yearly Average | | 1.25-2.0 | | 0.6-1.2 |
| | | Range $\mu L^{-1}$ | % decrease | Range $\mu L^{-1}$ | % decrease |
| 15 m | Aug-Oct | 3.5-7.0 | 0.25-1.5 | 4.0-6.0 | 0.25-1.6 |
| | Nov-Jan | 4.0-8.0 | 0.5-1.5 | 4.0-8.0 | 2.0-5.0 |
| | Feb-Apr | 2.75-3.5 | 2.0-4.25 | 2.75-3.75 | 2.0-5.0 |
| | May-Jul | 3..0-5.0 | 1.25-2.75 | 0-4.75 | 2.0-3.0 |
| | Yearly Average | | 1.0-3.0 | | 1.5-3.0 |
| | | Range $\mu L^{-1}$ | % decrease | Range $\mu L^{-1}$ | % decrease |
| 25m | Aug-Oct | 3.0-6.0 | 0.75-6.0 | 4.0-5.5 | 0.75-5.0 |
| | Nov-Jan | 2.5-7.0 | 0.5-0.70 | 4.0-9.5 | 0.5-7.0 |
| | Feb-Apr | 2.25-3.75 | 2.0-7.0 | 2.5-3.75 | 3.0-10.5 |
| | May-Jul | 2.5-4.5 | 2.0-6.0 | 2.5-4.0 | 2.0-6.5 |
| | Yearly Average | | 0.5-2.5 | | 0.5-3.5 |

| Farm Scenario 3 | Time | Pukehina | | Opotiki | |
|---|---|---|---|---|---|
| | Period | Range µL$^{-1}$ | % decrease | Range µL$^{-1}$ | % decrease |
| Surface waters | Aug-Oct | 4.5-7.0 | 0.4-1.0 | 4.5-6.0 | 0.5-0.5 |
| | Nov-Jan | 5.5-8.25 | 0.25-0.2 | 5.5-6.5 | 0-0.75 |
| | Feb-Apr | 2.5-3.25 | 2.5-4.0 | 2.5-3.25 | 1.5-3.0 |
| | May-Jul | 2.5-4.5 | 1.0-2.0 | 2.5-3.5 | 0.75-1.25 |
| | Yearly Average | | 5.0-8.0 | | 4.0-5.5 |
| | Period | Range µL$^{-1}$ | % decrease | Range µL$^{-1}$ | % decrease |
| 15 m | Aug-Oct | 3.5-7.0 | 0.6-1.5 | 4.0-6.0 | 0.2-0.5 |
| | Nov-Jan | 4.0-8.0 | 0.25-2.5 | 4.0-8.0 | 2.0-4.0 |
| | Feb-Apr | 2.75-3.5 | 2.5-5.5 | 2.75-3.75 | 2.0-4.0 |
| | May-Jul | 3..0-5.0 | 1.25-2.75 | 0-4.75 | 0.75-1.0 |
| | Yearly Average | | 1.0-2.75 | | 0.5-1.0 |
| | Period | Range µL$^{-1}$ | % decrease | Range µL$^{-1}$ | % decrease |
| 25m | Aug-Oct | 3.0-6.0 | 0.5-5 | 4.0-5.5 | 0.25-5.0 |
| | Nov-Jan | 2.5-7.0 | 0-8.0 | 4.0-9.5 | 0-1.0 |
| | Feb-Apr | 2.25-3.75 | 2.0-10.0 | 2.5-3.75 | 1.5-3.0 |
| | May-Jul | 2.5-4.5 | 2.0-6.5 | 2.5-4.0 | 1.0-1.5 |
| | Yearly Average | | 0.5-4.0 | | 0 |

### *3.2 FARMS SCENARIO*

Two farms were modelled during this simulation, a 5400Ha farm in a rectangular block offshore from Opotiki and a slightly smaller 4500Ha farm offshore from Pukehina (Figure 3.2)

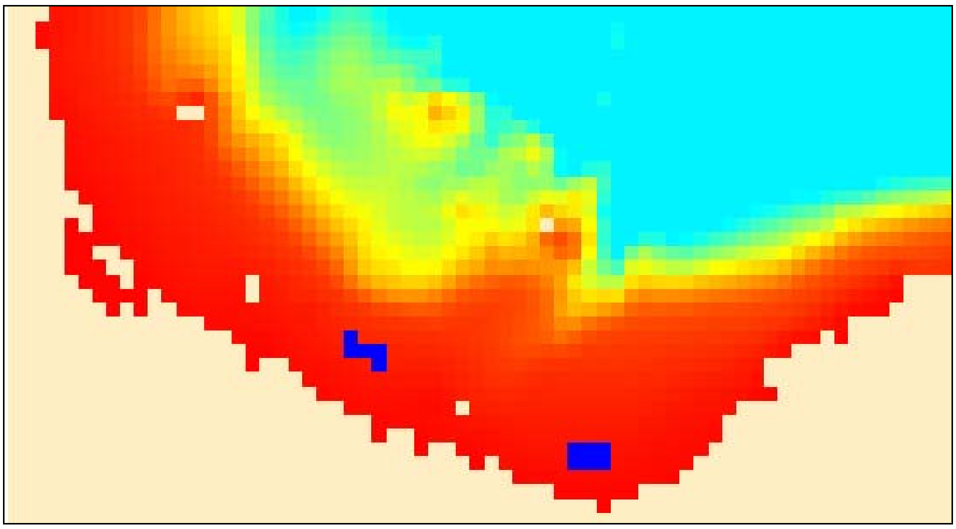

**Figure 3.2 –** Mussel farm locations offshore from Opotiki and Pukehina, 5400Ha and 4500Ha respectively. Farms shown in dark blue.

The model was run for the entire year (identical to the 'no farm' simulation) and the differences between the two runs calculated and averaged (Figures 3.3 to 3.6). Due to limited space, only selected plots are presented. Generally these are at the surface or at the depth range of 15-25 m (which is where the mussels are located in the model and where effects are likely to be greatest). Plots where seasonal effects are the greatest are also presented. Results of seasonal simulations at three depth layers (surface, 15 m and 25 m are presented in Table 3.1 - also refer to the CD-ROM attached to this report for full (seasonal) model outputs.

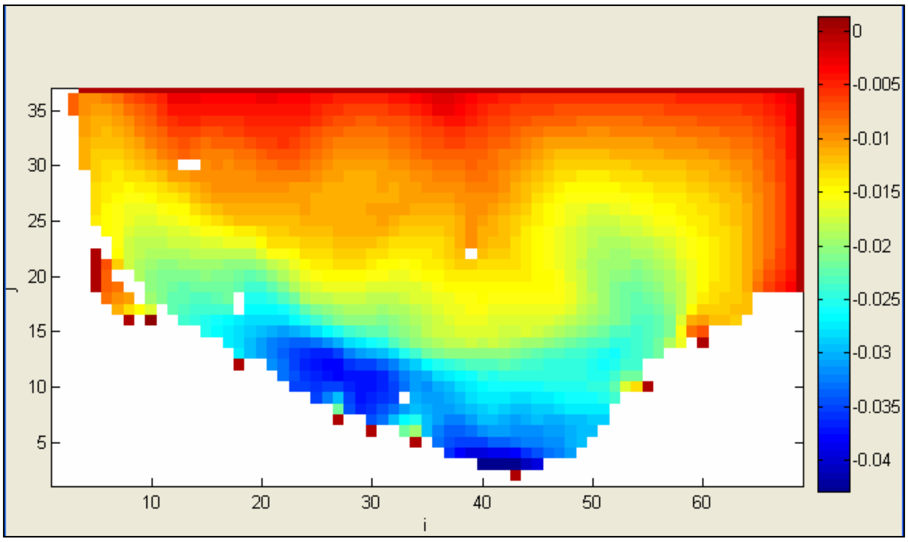


**Figure 3.3 –**Year long difference in the surface layer chlorophyll-a concentration ($mg/m^3$) between the 'no farm' and the '2 mussel farm' scenarios.

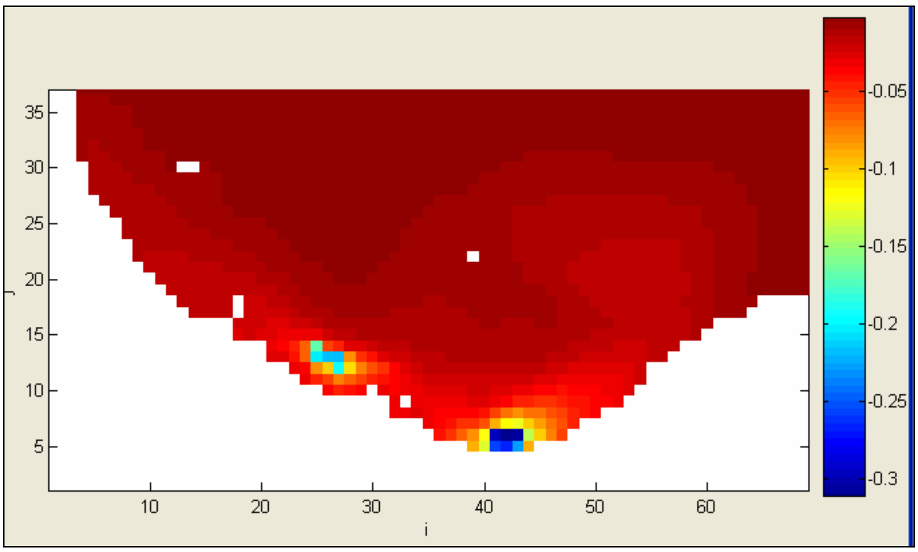


**Figure 3.4–**Year long difference in 15-25 m water depths of chlorophyll-a concentration ($mg/m^3$) between the 'no farm' and the '2 mussel farm' scenarios.

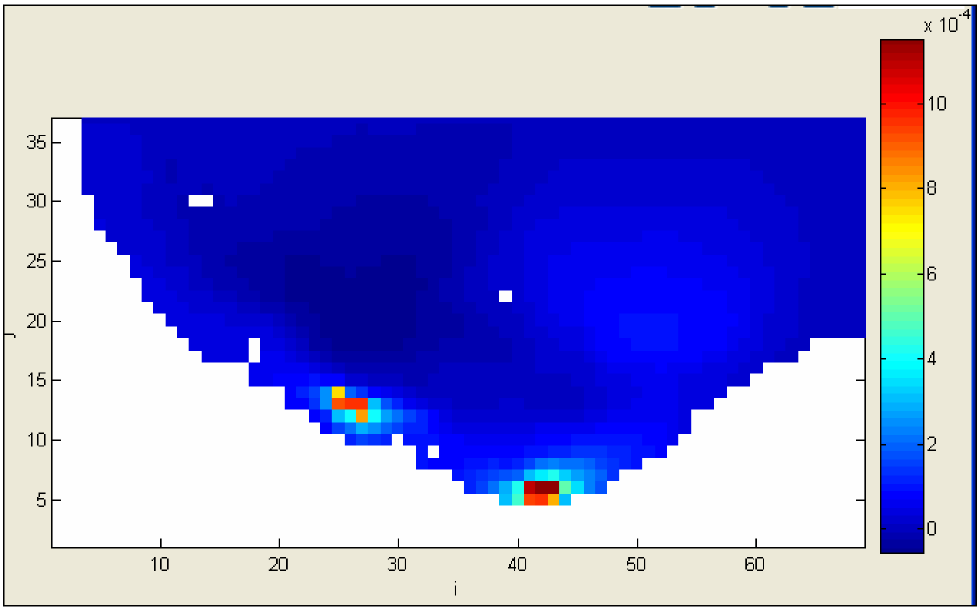


**Figure 3.5** - Year long difference in 15-25m water depths of ammonia concentration (g/m$^3$) between the 'no farm' model run and the '2 mussel farm scenario'. Note the local increase in ammonia as a result of excretion by the mussels.

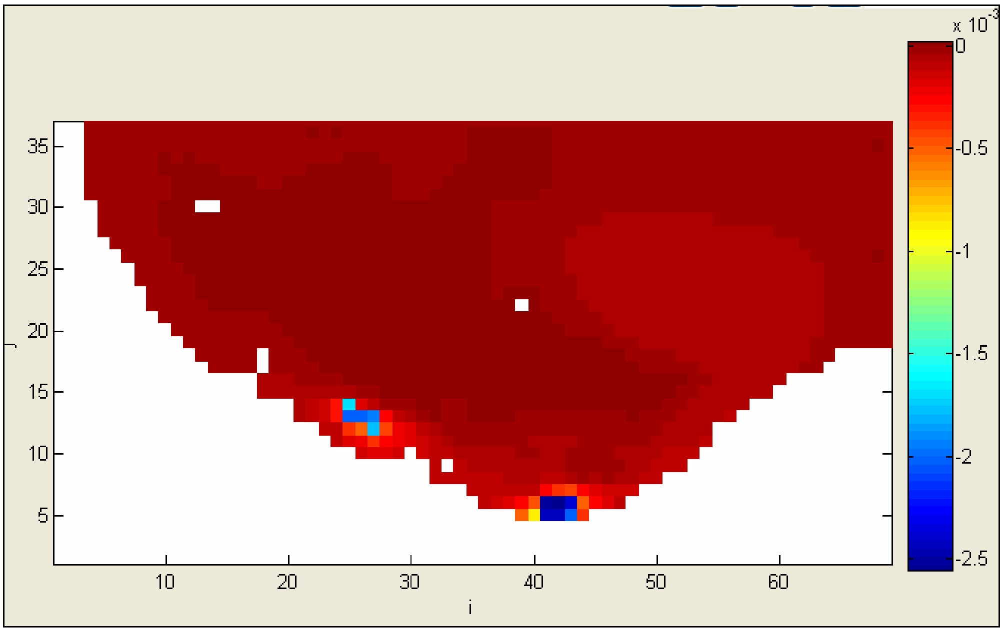


**Figure 3.6** - Year long difference in 15-25m water depths of dissolved oxygen concentration (g/m$^3$) between the 'no farm' model run and the '2 mussel farm scenario'.

It is apparent from the model runs that the two mussel farms are extracting phytoplankton, contributing ammonia, and extracting oxygen from the water column, as would be expected. The effects are greatest at the depth at which the farms are located and close to the farms themselves (Figures 3.3 to 3.6). Figure 3.3, showing the year long average difference in phytoplankton chlorophyll concentrations between the ‘no farm’ and ‘2 farm’ scenarios indicates that the effects of phytoplankton depletion may be apparent at a considerable distance from the farms as a result of the residual water currents transporting the ‘filtered’ water around the Bay.

The scale of this depletion however, must be considered. Figure 3.1 indicates the year long average phytoplankton chlorophyll-*a* value at the same location is ~4.5 mg/m$^3$. Thus, the depletion of phytoplankton at the water surface near the coast of Opotiki is approximately 1%. The year long differences in the water layer from 15 – 25 m (Figure 3.4) indicate changes of a larger magnitude, with reductions of approximately 8% in a zone that extends around the farms and to the coast inshore of the farms.

The largest decline of chlorophyll *a* in surface waters equates to a value of ~0.08 mg/m$^3$ (0.08 µg L$^{-1}$) near the coast at Opotiki and at Pukehina between Febuary and April. Effects are also greatest during this time period at 15 m depth where there is a reduction of 0.11 mg/m$^3$ at Opotiki and 0.07 mg/m$^3$ at Pukehina. Similarly, larger effects are evident at 25 m depth between Febuary and April with a reduction of 0.23 mg/m$^3$ at Opotiki and 0.34 mg/m$^3$ at Pukehina. The period between August and October, corresponds to the period of least impact, where Chlorophyll *a* is highest, which is a trend consistent among all depths at both Opotiki and Pukehina. Some depletion is compensated for by the increased ammonia inputs to the water column by mussel excretion, providing additional nutrient for phytoplankton growth – though the beneficial effect may vary with phytoplankton species.

Due to on average higher levels of coastal chlorophyll *a* on the shelf off Pukehina, this location is possibly the optimal area for farm productivity.

#### *3.2.1 FARMS LONGSHORE SCENARIO*

The four farm scenario oriented longshore from Pukehina to Opotiki (Figure 3.7) was tested to assess the impacts of broad-scale aquaculture oriented in an alongshore direction and to compare model results with a similar number of farms oriented in an offshore direction (see below). Three 4500Ha farms and a single 5400Ha farm offshore from Opotiki are simulated.

Water surface phytoplankton chlorophyll-*a* depletion (Figure 3.8) is greatest surrounding the farms and extends from around Maketu to Opotiki with magnitudes of ~ -0.07 mg/m$^3$. This value is approximately double the depletion value obtained with just two farms (Figure 3.3). Again at the water layer where the mussels are located, the impacts are more severe with reductions of 4-8% spreading along the coast. The vertical structure of the depletion (averaged over the entire year) is shown in Figure 3.10. Impacts of the farm on the depletion of phytoplankton decrease with increasing vertical and horizontal distance from the farm. The smaller reductions in phytoplankton are seen at a Bay-wide scale. While it appears that the impacts are less broadly spread at the 15-25 m depth than at the surface, a careful inspection of the colour scaling indicates that the spread of the smaller reductions is similar at both depths.

Similar temporal effects as the two farm scenario are evident in this simulation with highest depletions occurring between Febuary and April at all three depths examined. Chlorophyll-*a* depletion effects occur across the entire near-shore system. Reductions in the surface layer and at 15 m depth during this period range from 4-5 % of ambient chlorophyll-*a* levels, which equates to a decrease of ~ 0.15 to 0.18 mg/m$^3$. Largest reductions occur at 25 m depth with a 7 % decrease - 0.26 mg/m$^3$ at Pukehina and a 10 % - 0.375 mg/ m$^3$ at Opotiki.

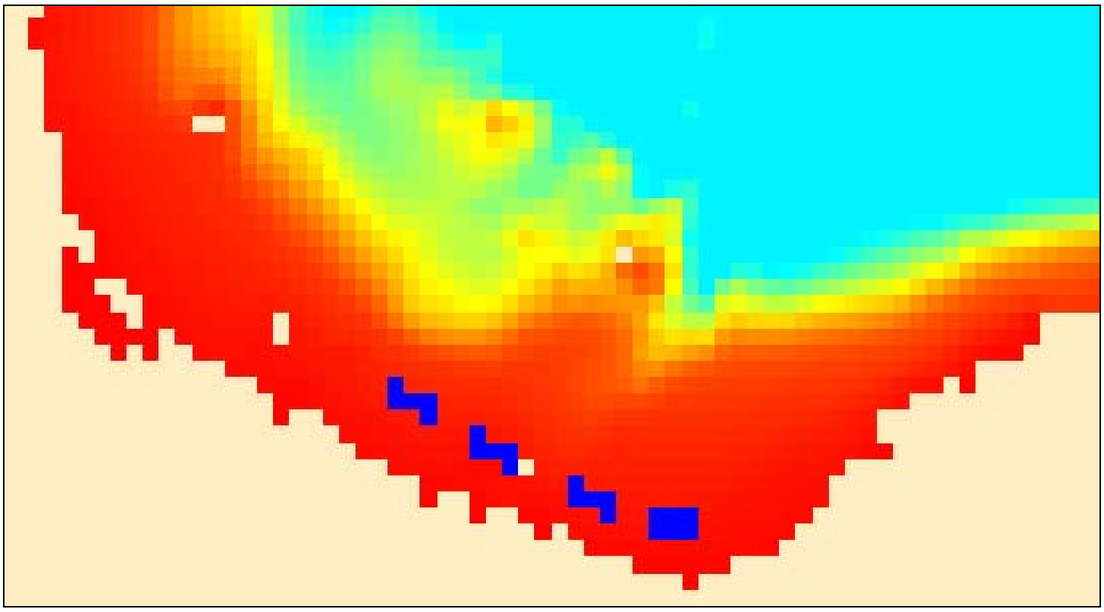

**Figure 3.7** – Mussel farm locations for the alongshore oriented aquaculture scenario. Three 4500Ha farms and a single 5400Ha farm offshore from Opotiki. Farms shown in dark blue

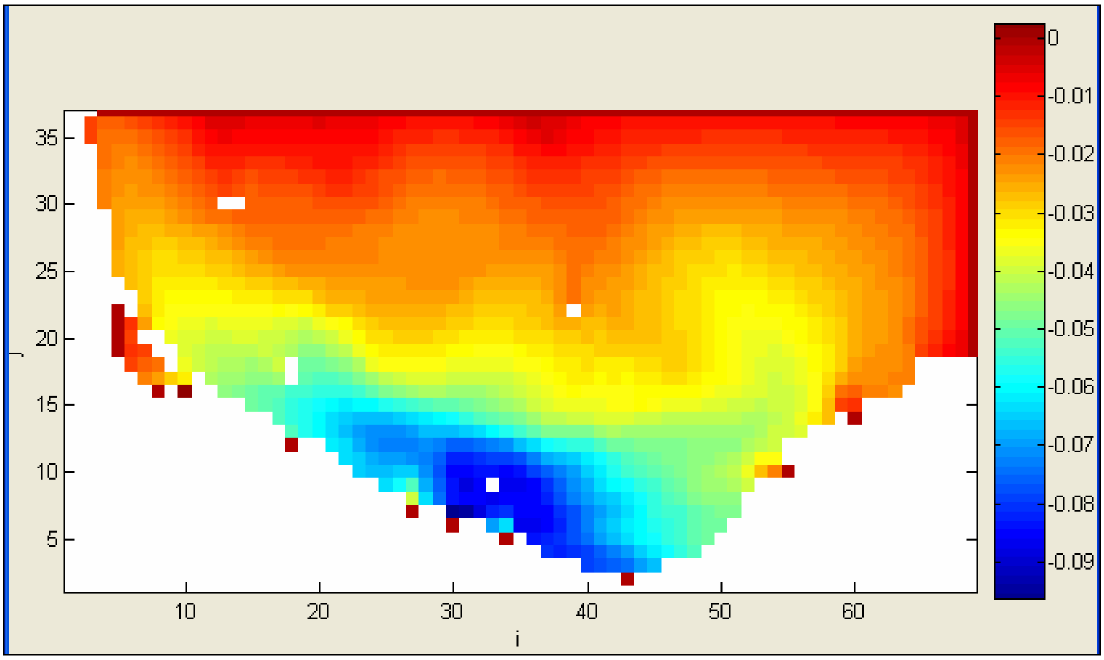


**Figure 3.8** - Year long difference in the surface layer chlorophyll-a concentration (mg/m$^3$) between the 'no farm' model run and the '4 farms alongshore scenario'.

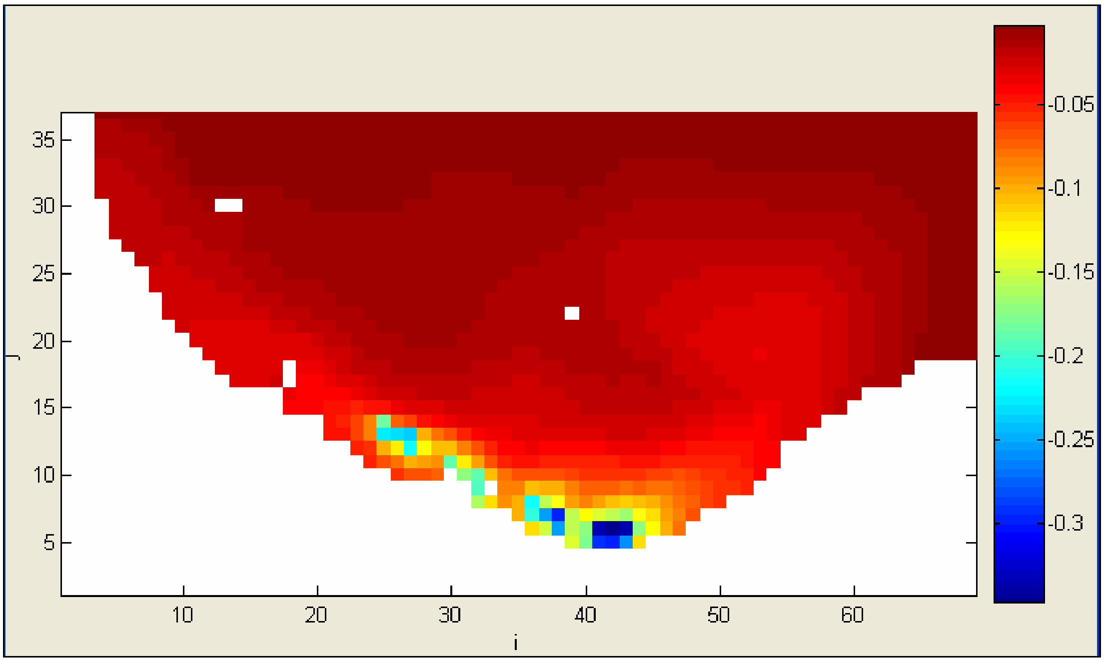


**Figure 3.9 -** Year long difference in the 15 – 25m water layer chlorophyll-a concentration (mg/m$^3$) between the 'no farm' model run and the '4 farms alongshore scenario'.

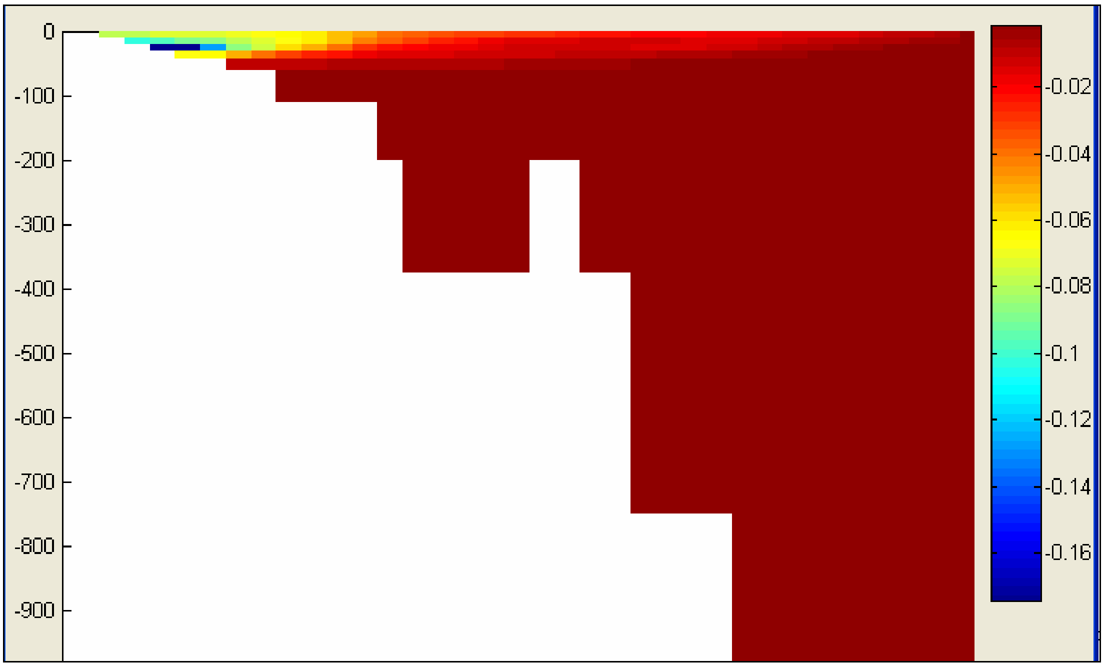


**Figure 3.10 -** Year long difference in water layer chlorophyll-a concentration (mg/m$^3$) on an offshore transect off Opotiki between the 'no farm' model run and the '4 farms alongshore scenario'. Note the highest depletion is located in the water layers where the farm is located (15-25 m) with impacts declining both horizontally and vertically away from this area.

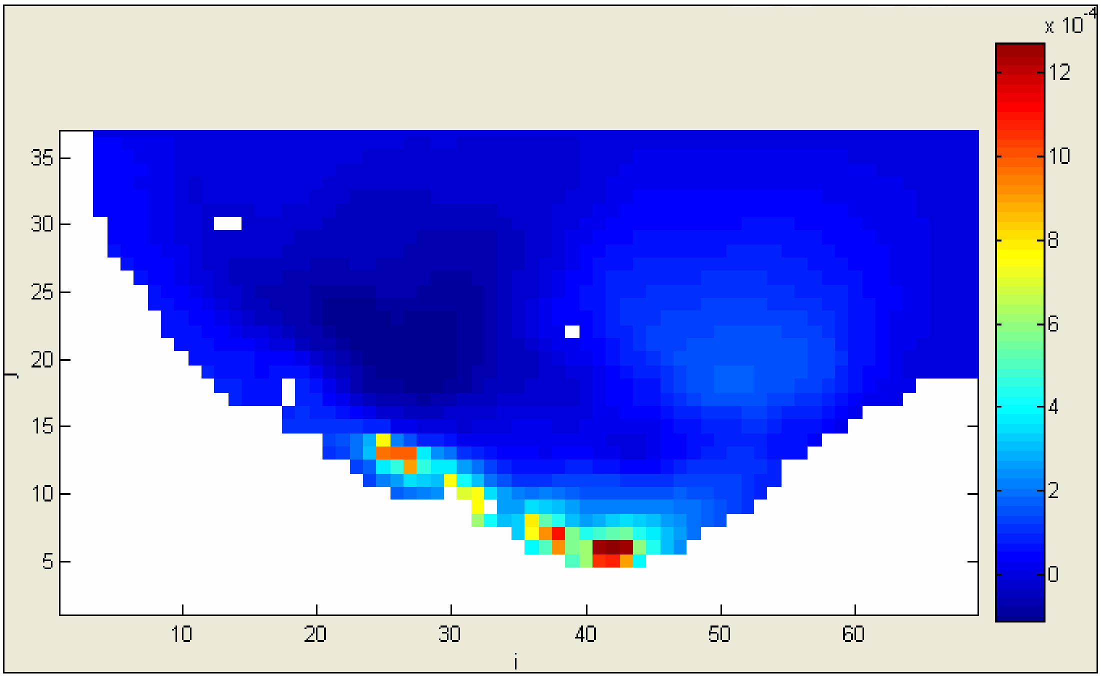


**Figure 3.11** - Year long difference in the 15 – 25m water layer ammonia concentration (g/m$^3$) between the 'no farm' model run and the '4 farms alongshore scenario'.

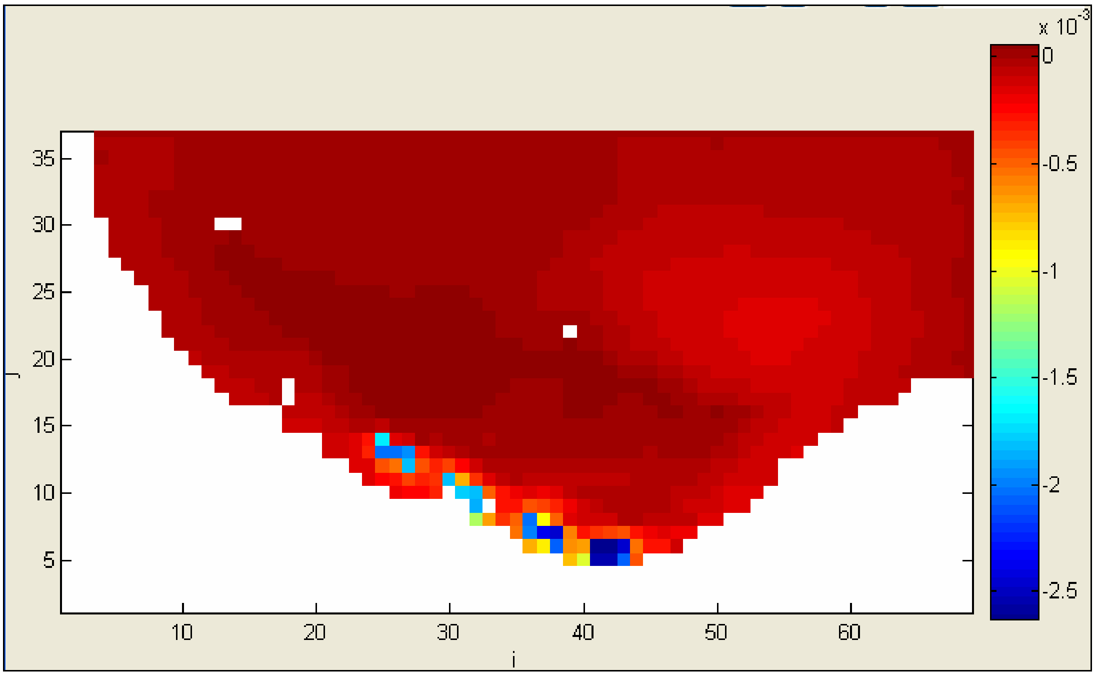


**Figure 3.12** - Year long difference in the 15 – 25m water layer dissolved oxygen concentration (g/m$^3$) between the 'no farm' model run and the '4 farms alongshore scenario'.

### 3.2.2 FARMS CROSS-SHORE SCENARIO

The second four farm scenario (Figure 3.13) was tested to assess the impacts of wide-scale aquaculture oriented in the cross-shore direction near Pukehina and to compare model results with a similar number of farms oriented in the longshore direction (above).

Overall the spatial extent of the depletion zone is smaller (Figure 3.14) than that of 4 farms located in an alongshore direction (Figure 3.8) whereas at 15 and 25 m depth the extent of depletion is of higher magnitude than at the surface. Increases in water column ammonia concentrations (Figure 3.16) are of similar magnitude to those farms located in the alongshore direction (Figure 3.11), as are water column depletions of dissolved oxygen concentrations (Figure 3.17 and 3.12).

Mirroring trends above, highest chlorophyll *a* depletions occur in the surface water and at 15 m and 25 m depth between February and April when chlorophyll-*a* levels are at their lowest. Not surprisingly, higher reductions occur around Pukehina than at Opotiki. Surface water depletions equate to a 4 % (0.13 $\mu g/m^3$) reduction at Pukehina and a 3 % (0.098 $\mu g/m^3$) reduction at Opotiki. Reductions at 15 m depth are ~ 5 % (0.19 $\mu g/m^3$) at Pukehina and 4 % (0.15 $\mu g/m^3$) at Opotiki. However, highest reductions ~ 10 % (0. 38 $\mu g/m^3$) occur at 25 m depth at Pukehina.

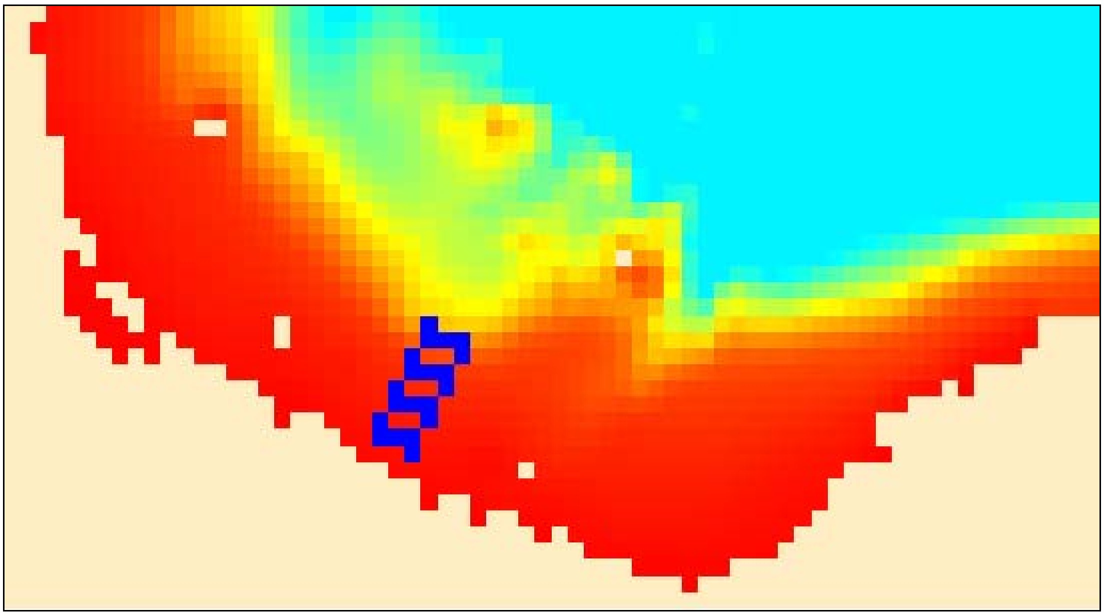

**Figure 3.13 -** Mussel farm locations for the offshore oriented aquaculture scenario. Four 4500Ha farms are simulated offshore from Pukehina. Farms shown in dark blue

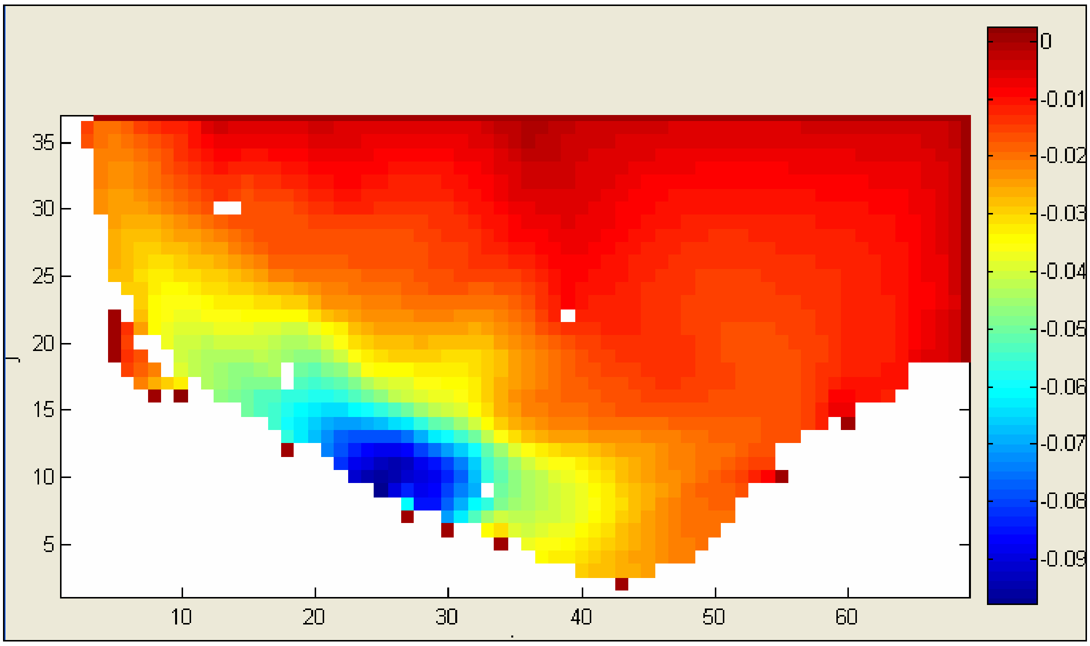


**Figure 3.14 -** Year long difference in the surface layer chlorophyll-a concentration (mg/m$^3$) between the 'no farm' model run and the '4 farms cross-shore scenario'.

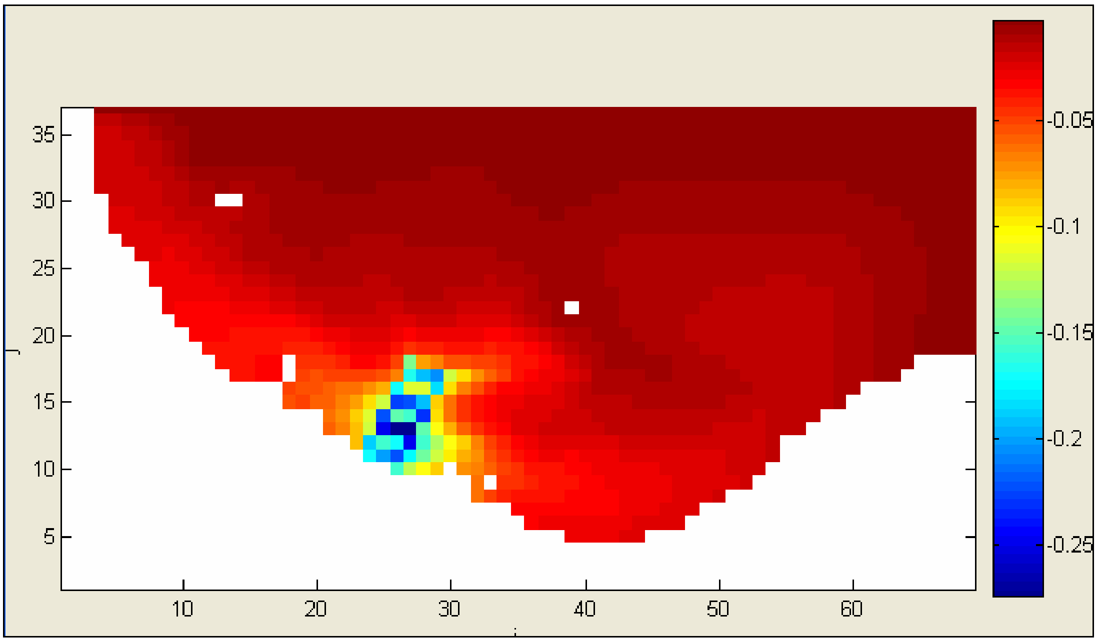


**Figure 3.15 -** Year long difference in the 15 – 25m water layer chlorophyll-a concentration (mg/m$^3$) between the 'no farm' model run and the '4 farms cross-shore scenario'.

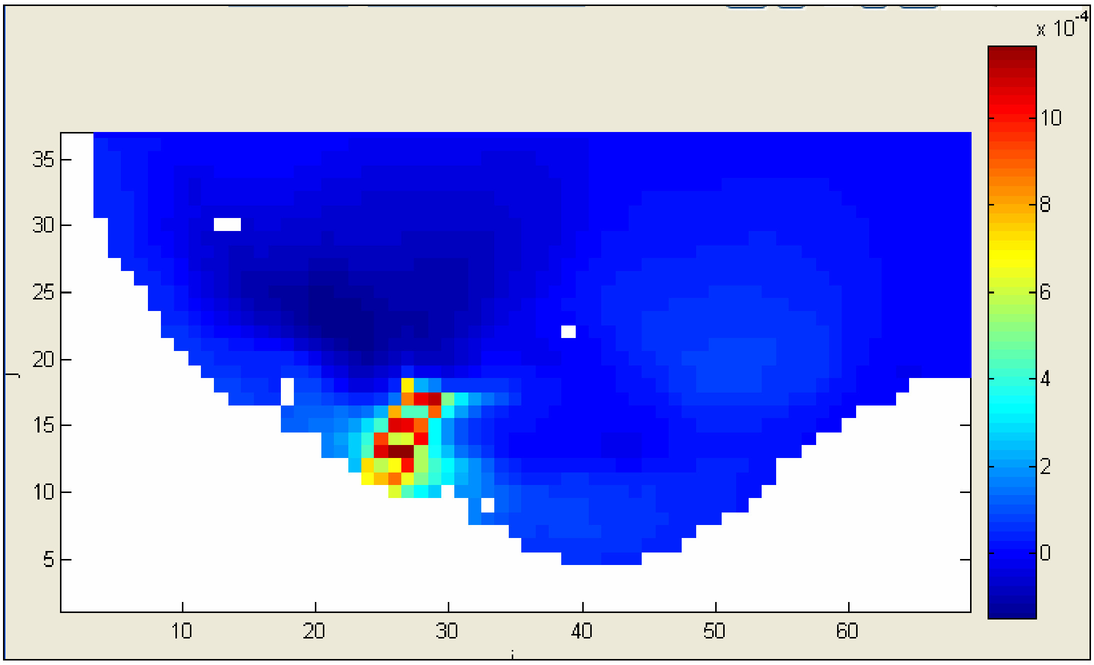


**Figure 3.16 -** Year long difference in the 15 – 25m water layer ammonia concentration (g/m$^3$) between the 'no farm' model run and the '4 farms cross-shore scenario'.

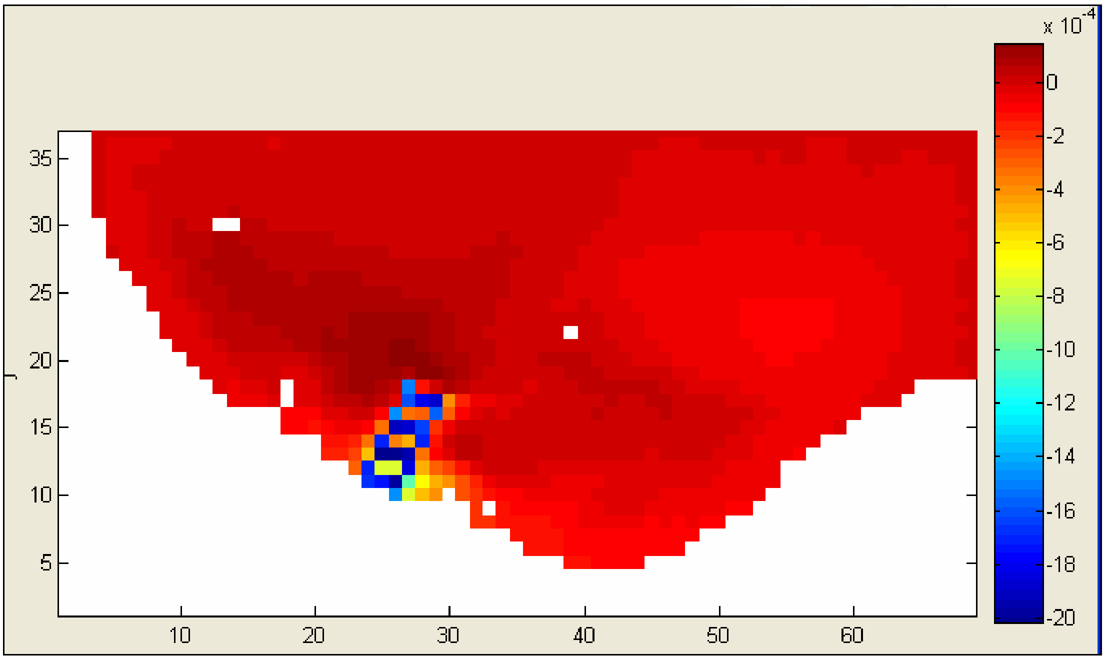


**Figure 3.17 -** Year long difference in the 15 – 25m water layer dissolved oxygen concentration (g/m$^3$) between the 'no farm' model run and the '4 farms cross-shore scenario'.

# 4 ECOLOGICAL IMPLICATIONS

## *4.1 CARRYING CAPACITY*

Within the ecological literature there are multiple definitions for carrying capacity in relation to bivalve culture and equally different empirical approaches that have been used for determining carrying capacity (Dame *et al.* 1997; Prins *et al.* 1998, Smaal *et al.* 1998; Telfor and Robinson 2003; Jiang and Gibbs 2004**.** For the purposes of this study we define carrying capacity in terms of production carrying capacity and ecological carrying capacity. Maximum production carrying capacity has been described as the maximum level of bivalve culture, which replaces the ecological role of zooplankton, whereby the ecosystem is reduced to a nutrient–phytoplankton–culture–detritus system with the absence of zooplankton (Jiang and Gibbs 2004). In the absence of zooplankton, higher trophic levels dependent on zooplankton are not present. On the other hand, ecological carrying capacity has been defined as the stocking or farm density which causes unacceptable ecological impacts (Inglis *et al.* 2005). Jiang and Gibbs (2004) further define ecological carrying capacity as the level of culture that can be achieved without changing the major energy fluxes of structure of the food web. In their review, Prins *et al.* (1998) propose that carrying capacity for exploitation should be evaluated both on the scale of a system and on a local scale. Ecosystem-scale carrying capacity generally is determined by food production and import while local-scale carrying capacity is determined by physical factors such as substrate types, currents and shelter.

The appropriate determination of carrying capacity for a given body of water (farm, embayment and/or region), therefore requires understanding of the distribution and abundance of dominant species and general community composition (benthic and pelagic), including trophic level energy requirements and likely impacts to these systems. Information of this nature is often lacking for many systems.

## *4.2 PRODUCTION CARRYING CAPACITY*

Based on the existing 3DDLife modelling simulations, chlorophyll-*a* is patchily distributed through space and time throughout the Bay of Plenty, but is typically higher in near-shore areas relative to off-shore areas. On average, chlorophyll-*a* is highest between August and January and lowest between February and April in surface waters and at both 15 and 25 m depth (Table 3.1). Moreover, chlorophyll-*a* is typically lower at Opotiki than the Pukehina coastal area (Table 3.1).

The farm configurations that pose the largest impacts to chlorophyll-*a* depletion and thus production carrying capacity within the coastal Bay of Plenty system are the 2 four farm scenarios. Nevertheless, on a seasonal basis, depletions within all farm scenarios are localised and relatively low. The largest effects are likely to occur in coastal surface waters between February and April when chlorophyll-*a* is at its minima with reductions of 3.5-4.0 % around Opotiki and Pukehina. Reductions of this scale correspond to a very small decrease in Chlorophyll-*a*, i.e., a maximum reduction of 0.126 µg $L^{-1}$ around Pukehina and at Opotiki respectively (Table 3.1). Similarly, at 15 m depth largest reductions are likely to occur between February and April and also equate to small decreases in chlorophyll-*a*, e.g. < 0.2 µg $L^{-1}$. Of all the depth strata and scenarios examined, largest decreases in chlorophyll *a* occur at 25 m depth between February and April with a 9 % reduction at Opotiki (Scenario 1) a 10 % reduction in Chlorophyll-*a* at Opotiki (Scenario 2) and a 10 % reduction at Pukehina (Scenario 3). Again, these percentage-wise reductions correspond to small decreases in Chlorophyll-*a* with maximum reductions in the range of 0.2- 0.4 µg $L^{-1}$.

In relation to production carrying capacity, Inglis *et al.* (2005) provide generic guidelines for phytoplankton abundance in concert with water velocity requirements for sustainable mussel aquaculture (see Box 1 –Inglis *et al.* 2005; Box 1). These values are in general agreement with other studies e.g., Hawkins *et al*. (1999) observed wasting of mussels at chlorophyll concentrations below 0.86 µg $L^{-1}$, and no significant growth below 1 µg $L^{-1}$. Similarly, the critical chlorophyll concentration for mussel growth in Pelorous Sound has been found to be between 1 µg $L^{-1}$ (Ross *et al*., 1998) and 1.5 µg $L^{-1}$ (Waite, 1989).

Comparing values obtained from the 3DDlife modelling (following conversion to comparable units) with Inglis *et al.* (2005) (Box 1), phytoplankton in coastal waters in the Bay of Plenty would be well in excess of that required for mussel growth (scenarios 1 to 3) . Even during times of lowest Chlorophyll-*a* concentrations (late summer/autumn), which range from 2.5 µg $L^{-1}$ to 3.75 µg $L^{-1}$ among depths, it is unlikely that mussel growth will be limited in surface waters, at 15 m depth, or 25 m depth.

The next questions to consider are what are the likely effects on the ecological carrying capacity of the Bay of Plenty ecosystem, resulting from the loss of plankton depicted from the modeling?

**Box 1:** Guidelines for levels of phytoplankton abundance and water velocity for sustainable mussel culture defined by Inglis *et al*. (2005)

**Food levels**

• *Chlorophyll <0.5* µ*g/l* – very poor growing conditions, very slow growth and loss of condition if for a prolonged period
• *Chlorophyll in range 0.5-1* µ*g/l* – generally poor growing conditions. Mussels grow slowly and may not lose condition, but recovery following spawning is slow, and it takes a long time to reach harvestable size.
• *Chlorophyll in range 1-2* µ*g/l.* Moderate growing conditions, mussels of reasonable condition if interspersed with periods of higher chlorophyll concentration.
• *Chlorophyll in range 2-4* µ*g/l.* Good growing, likely to achieve harvestable size in 10-12 months. Mussels should achieve good condition with rapid recovery from spawning.
• *Chlorophyll in range 4-8* µ*g/l.* Ideal growing conditions. Likely to be rare, fast growth.
• *Chlorophyll > 8* µ*g/l.* Little known, could be good growing but food handling difficulties.

**Water currents**

• *Velocity <5 cm/s.* - very weak current, poor mass flux and inconsistent current direction. Depletion likely at the centre of farms. Only suitable for low density farming or spat holding.
• *Velocity 5-10cm/s.* - weak current velocities of generally widely varying direction leading to some depletion at centre of farm.
• *Velocity 10-20cm/s.* - moderate-low depletion that may be more marked at downstream end of farm. Depletion is more likely to be observed in centre of farmed area.
• *Velocity >20cm/s.* - strong current flow. Little depletion but cumulative effect of many ropes/longlines in the direction of flow could result in depletion.

### *4.3 ECOLOGICAL CARRYING CAPACITY*

To date, there have been limited studies on ecological carrying capacity thresholds in relation to aquaculture i.e., percentage-wise reductions in chlorophyll-*a* that will invoke negative impacts to existing levels of flora and fauna in a defined system. Of those studies done, many have been concerned with estimating carrying capacity for small embayments (e.g., Telfor and Robinson 2005) rather than larger coastal areas, as is the case for the present study. In their study of the carbon budget for Killary Harbour, Ireland, Rodhouse and Roden

(1987) predicted that when greater than 50 % of the primary productivity of the embayment is diverted to mussel-rearing, significant modifications of the environment and decreased production yield may occur. Inglis *et al.* (2005) suggest there is minimal empirical basis for this figure, as natural rates of primary production are extremely variable in space and time.

In terms of evaluating ecological carrying capacity of a system relative to mussel aquaculture within New Zealand, the most comprehensive modeling has been that of Jiang and Gibbs (2004), where the carrying capacity of bivalve shellfish culture in the Tasman/Golden Bays was tested using the steady, linear food web model ECOPATH (Christensen *et al.* 2000). Briefly, the outputs of this model produce two measures of carrying capacity including production carrying capacity, and the ecological carrying capacity. Predetermined boundary states representative of the carrying capacity limits are defined and used to determine the level of culture that would reach boundary limits. The model relies on key ecosystem components based on a wide range of data from fisheries estimates of biomass down to phytoplankton abundance, which are placed into discrete compartments. For each compartment, the user supplies estimates of average annual biomass, production/biomass, consumption/biomass, ecotrophic efficiency (the proportion of a compartment which is utilized within the ecosystem), diet composition (what other compartments are exploited) and exports from the system. The model identifies how strongly linked the compartments are and allows the carrying capacity of the system to be assessed in relation to perturbations e.g., those associated with marine farming. However, the model does not take into account seasonal fluctuations in species abundances or depth-related impacts as those produced by the current 3DDLIFE productivity simulations.

### *4.4 EFFECTS ON ECOSYSTEM CARRYING CAPACITY*

While detailed empirical evaluation of the ecosystem carrying capacity of the Bay of Plenty System requires further examination, which was outside of the general scope of this study, based on the existing information obtained from the first-order ecological study (Mead *et al.* 2005), detailed analysis of hydrology (Black *et al.* 2005) and the results of the productivity modelling (this report) it is unlikely that the present ecological carrying capacity, in terms of altering the major energy fluxes or structure of the food web would be adversely affected by the proposed marine farming.

The principle reasons for this assertion is that maximal rates of phytoplankton reduction relative to the modelled scenarios are generally small and the resulting chlorophyll-*a* levels are well in excess of those required for sustaining mussel growth (Inglis *et al.* 2005). Within the Bay of Plenty system, nutrients utilised by phytoplankton are provided by both riverine inputs and nutrient-rich deeper water upwelling to the coast. In other words, the system is not closed, as is the case for other locations within New Zealand subject to intensive farming that have concerns with carrying capacity e.g., Beatrix Bay Marlborough Sounds. Beatrix Bay is largely mediated by poor flushing with nutrient limitation magnified in particular areas (e.g., at the heads of bays) due to low currents (i.e. poor circulation and flushing, re-circulating eddies, *etc*.). A fundamental aspect of good mussel farm location is the requirement of high current flow (as in the present case) because high currents and good circulation provide a larger volume of water to filter food from, reduce impacts on the immediate seabed and mix the locally-high chlorophyll levels. Areas of slow currents are more likely to incur benthic impacts (Inglis *et al.* 2005) and receive less food (Black *et al.* 2001).

### *4.5 IMPACTS ON THE FOOD WEB*

Considering the present modeled chlorophyll-*a* in relation to the three farming scenarios, it is unlikely that the depletion of phytoplankton over ranges depicted will significantly alter the structure of zooplankton assemblages and any impacts are to likely be localised. Estimates of chlorophyll-*a* concentrations at which herbivorous zooplankton growth and survival is compromised varies considerably among species. For example, many zooplankton (e.g., copepod and cladoceran species) have lower limits of growth between 0.2- 1 μg $L^{-1}$ (Frost 1975; Peters and Downing 1984; Paffenhöfer and Orcutt 1986; Kleppel 1993), values that are still likely to be in existence in the Bay of Plenty for all seasons and depths under all modeled scenarios. For the Tasman/Golden Bay ecosystem, Jiang and Gibbs (2005) suggest that of the total primary production in that system, roughly half is consumed by zooplankton, whilst the remainder flows to detritus and is recycled. As many coastal systems within New Zealand are dominated by primary productivity and assuming this relationship is somewhat analogous to the Bay of Plenty system, it is hard to envisage that the ecological carrying capacity would be compromised by the level of aquaculture investigated here.

For the most part, the study area (Between Tauranga and Waihau Bay) is dominated by soft sediment habitats (Mead *et al.* 2005). Bottom complexity/types include rippled gravel and shell-lag to depths of 10-40 m in the western part of the survey area, finer sands and silt to the east of Ohope extending into the shallow areas (10 m), with a band of higher habitat complexity west of the central part of the survey area (associated with the offshore islands), and 3 areas of reef between 10 and 30 m deep. Polychaetes and amphipods are the dominant fauna in the area although, species distributions are inherently patchy. Amphipods occur in higher numbers in the shallower (< 50 m) mud/silt areas, while polychaetes dominate sandy areas with high organic content, which are concentrated in the north-western parts of the survey area. A wide variety of bivalves are spread throughout region including *Nucula* spp., *Dosinia* spp., and low numbers of pipi (*Paphies australis*), scallops (*Pecten novaezelandiae)* and the morning star shell *Tawera spissa*. Echinoderms (brittle stars and sea cucumbers) and foramiferans were also fairly common, with the former being widely distributed and the latter being restricted to deeper survey sites. Inglis et al (2005) suggest that while mussels have an inherent ability to survive periods of low phytoplankton abundance, this may not be true for other marine organisms within the same system. Little information is available on likely effects of marine farming to existing biological populations; however, considering the composition of benthic organisms and lack of rocky reef habitat within the Bay of Plenty area (Mead *et al.* 2005), it is unlikely that the marine farming will impose large-scale negative impacts to existing flora and fauna.

Despite the existence of comprehensive Chlorophyll *a* modeling, one aspect that is unknown for the present situation and that is generally overlooked or deemed difficult to appraise in other studies, is how the proposed aquaculture activity will affect phytoplankton species composition through space and time including potential effects this may have on production and ecosystem carrying capacity.

While information on chlorophyll composition through space and time is limited for the Bay of Plenty area, studies in the Hauraki Gulf, north-eastern New Zealand have demonstrated the type of seasonal fluctuations that can occur. Chang *et al.* (2003) documented seasonal changes in the nature of the phytoplankton community of the open coastal and Gulf waters thought to be driven by the seasonal changes in physico-chemical conditions. During spring, the inner-shelf region of the open coastal waters support a high biomass community of large, chain-forming diatoms. As nitrogen becomes depleted, this gives way to a community of smaller diatom species and eventually to a mixed community of small diatoms, dinoflagellates, small phytoflagellates and picophytoplankton late in the summer. Farther offshore, the (relatively nutrient-poor) outer shelf waters harbour lower phytoplankton biomass dominated by small, motile taxa throughout the spring and summer. Within the Hauraki Gulf, the phytoplankton community is dominated by larger, autotrophic dinoflagellates in spring, but later in the year these are replaced by smaller autotrophic and heterotrophic dinoflagellates, nanoflagellates and picophytoplankton.

Further assessments of the ecosystem carrying capacity can be achieved by additional modelling and investigating present knowledge gaps, particularly the variation in phytoplankton species composition through space and time within the Bay of Plenty and impacts on the zooplankton community. Other factors that also impact on ecosystem health and warrant investigation are the significance of zooplankton mortality due to marine farms with respect to recruitment of other water-borne marine organisms and the potential impacts of mussel spat colonisation to new locations outside the marine farms (resulting to a decreased of marine biodiversity and/or community change).

Considering mussels are selective feeders, knowledge of phytoplankton species composition (size fractions) and the potential for toxic algal outbreaks (e.g., Chang *et al*. 1996) through space and time within the Bay of Plenty will also be of importance. While this study has focused on mussel culture to investigate aquaculture-related effects on primary production and production carrying capacity in the Bay of Plenty, it is acknowledged that the AMAs could be used for other types of aquaculture. Mussels have been used because impacts related to mussel aquaculture have been relatively well studied compared to other aquaculture types in New Zealand. Effects of other of aquaculture “types” will depend on the species being cultivated, relative stocking densities and the water depth being utilised.

## 5 SUMMARY

The potential effects of several large aquaculture farms within the Bay of Plenty have been simulated with a calibrated ecological model. The model has advantages over more conventional models as it allows detailed examination of water-column dynamics among different depth strata, thus comprehensive examination of potential effects; in this case effects on primary production. Maximal impacts of two large mussel farms (4500 Ha and 5400 Ha) and two different arrays of four mussel farms located in the Bay of Plenty suggest higher impacts are mostly restricted to the environs of the farm and the adjacent coast.

Irrespective of the farm array, impacts to chlorophyll *a* levels are greater in late summer (February-April) when ambient levels of phytoplankton are at their minima. Larger impacts are evident at the depth layer in the water column where the mussels are located, i.e., between 15-25 m depth. Over an annual period the mussel farms may enhance the local ammonia concentration by approximately 0.001 $g/m^3$, and deplete the local dissolved oxygen concentration by approximately 0.002 $g/m^3$, relative to background values of ~0.05 $g/m^3$ and 8 $g/m^3$ respectively.

It is unlikely that the production carrying capacity of the Bay of Plenty system will be adversely affected by the level of aquaculture modelled in this study, as even maximum depletion rates resulted in chlorophyll-*a* levels well above published threshold production carrying capacity levels identified for mussel farming in other parts of New Zealand, e.g., ~ 1 $\mu g\ L^{-1}$. Given the physical and biological characteristics of the Bay of Plenty area, relative to the predicted levels of impact presented here, it is also unlikely that the ecosystem carrying capacity will be adversely affected. Further assessments of the ecosystem carrying capacity can be achieved by additional modelling and investigating present knowledge gaps, particularly the variation in phytoplankton species composition through space and time within the Bay of Plenty.

# 6 REFERENCES


Black, K.P., Mead, S.T., Longmore, A. 2001 The Sustainability of Marine Farming in Beatrix Bay, Marlborough Sounds. Report prepared by ASR Consultants for the Marlborough Sounds Trust, March 2001.

Black, K.P., Beamsley, B., Longdill, P,. Moores, A. 2005 Current and Temperature Measurements: Aquaculture Management Area. Report prepared by ASRConsultants for Bay of Plenty Regional Council, March 2005.

Bowie, G.L., Mills, W.B., Porchella, D.B., Campbell, C.L., Pagenkopf, J.R., Rupp, G.L., Johnson, K.M., Chan, P.W.H., and Gherini, S.A. 1985. Rates, Constants, and Kinetics Formulations in Surface Water Quality Modeling (2nd ed.). Tetra Tech Inc. Lafayette, California. EPA/600/3-85/040 Environmental Reaserch Laboroatory, Office of Research and Development, U.S. Environmental Protection Agency, Athens, Georgia. 455p.

Chang, F.H., Sharples, J., Grieve, J.M. 1996. Temporal and spatial distribution of toxic dinoflagellates in Bay of Plenty, New Zealand, during the early 1993 toxic shellfish outbreaks . Harmful and Toxic Algal Blooms. pp. 235-238.

Chang, H.F., Zeldis, J., Galll, M., Hall, J. 2003. Seasonal and spatial variation of phytoplankton assemblages, biomass and cell size from spring to summer across the north-eastern New Zealand continental shelf. *Journal of Plankton Research* 25: 737-758

Christensen, V., Walters, C.J., Pauly, D., 2000. Ecopath with Ecosim: a User's Guide, October 2000 Edition. Fisheries Centre, University of British Columbia, Vancouver, Canada and ICLARM, Penang, Malaysia. 130 pp.

Dame, R.F. Prins, T.C. 1998 Bivalve Carrying Capacity in Coastal Ecosystems. *Aquatic Ecology* 31: 409-421.

Eppley, R.W., 1972. Temperature and phytoplankton growth in the sea. *Fisheries Bulletin* 70. 1063-1085.

Hawkins, A.J.S., James, M.R., Hickman, R.W., Hatton, S. and Weatherhead, M. 1999. Modelling of suspension-feeding and growth in the green-lipped mussel *Perna Canaliculus* exposed to natural and experimental variations of seston availability in the Marlborough Sounds, New Zealand. *Marine Ecology Progress Series* 191: 217-232.

Inglis, G.J., Hayden, B.J., Ross, A.H. 2000. An overview of factors affecting the carrying capacity of coastal embayments for mussel culture. Report for Ministry for the Environment No. MFE00505

James, M.R., Weatherhead, M.A., Ross, A.H., 2001. Size-specific clearance, excretion, and respiration rates, and phytoplankton selectivity for the mussel *Perna canaliculus* at low levels of natural food. *New Zealand Journal of Marine and Freshwater Research*. (35) 73-86.

Jiang, W., Gibbs, M.T. 2005. Predicting the carrying capacity of bivalve shellfish culture using a steady, linear food web model. *Aquaculture* 244: 171– 185

Kleppel, G.S. 1993. On the diets of calanoid copepods. *Marine Ecology Progress Series* 99: 183-195.

Longdill, P.C., Black, K.P., Park, S. and Healy, T.R., 2005. *Bay of Plenty Shelf Water Properties Data Report 2003 – 2004: Aquaculture Management Areas.* Report for Environment Bay of Plenty, ASR Ltd, P.O. Box 67, Raglan, NZ, and the University of Waikato. 35p.

Longdill, P. C., and Black, K. P., 2006. *Numerical hydrodynamic modelling: Aquaculture Management Areas.* Report for Environment Bay of Plenty, ASR Ltd, P.O. Box 67, Raglan, NZ, and the University of Waikato. 53p.

Marsden, I.D., and Weatherhead, M.A., 1999. Shore-level induced variations in condition and feeding of the mussel *Perna canaliculus* from the east coast of the South Island, New Zealand. *New Zealand Journal of Marine and Freshwater Research*. (33) 611-622.

Mead, S.T., Longdill, P., Moores, A., Beamsley, B., Black, K.P., 2005 Bay of Plenty Biological Survey: Aquaculture Management Area. Report prepared by ASR Consultants for Bay of Plenty Regional Council, March 2005.

Paffenhöfer, G.A., Orcutt, J.D. 1986. Feeding, growth and food conversion of the marine cladoceran *Penilia avirostris*. *Journal of Plankton Research* 8(4): 741-754.

Park et al. 2006 AMA survey report ENVBOP

Peters, R.H., Downing, J.A. 1984. Empirical analysis of zooplankton filtering and feeding rates. *Limnology & Oceanography* 29(4): 763-784.

Prins, T. C, Smaal, A. C., Dame, R. F. 1998. A review of feedbacks between bivalve grazing and ecosystem processes. *Aquatic Ecology* 31: 349-359.

Reeve, M.R., Walter, M.A. 1977. Observations on the existence of lower threshold and upper critical food concentrations for the copepod *Acartia tonsa* Dana. *Journal of Experimental Marine Biology and Ecology* 29: 211-213.

Rodhouse, P.G., Roden, C.M. 1987. Carbon budget for a coastal inlet in relation to intensive cultivation of suspension-feeding bivalve molluscs. *Marine Ecology Progress Series* 36: 225-236.

Ross, A.H., James, M.R., Hadfield, M. and Gibbs, M. 1999. *Estimating the sustainable production of mussel aquaculture using numerical simulation models.* International Conference on Sustainable Management of Coastal Ecosystems, Oporto, Portugal (abstract).Smaal, A. C., Prins, T. C., Dankers, N., Ball, B. 1998. Minimum requirements for modelling bivalve carrying capacity. *Aquatic Ecology* 31: 243-428.

Steele, J.H., 1965. Notes on some theoretical problems in production ecology. In, *Primary production in aquatic environments*. C.R. Goldman (ed.). University of California Press, Berkely, California, pp393-398.

Taylor, J.R., and Park, S.G., 2001. *Natural Environmental Monitoring Network: Bay of Plenty Rivers' Water Quality 1989 – 2000*. Environment B.O.P Environmental Report 2001/12, April 2001.

Telfor, T., Robinson, K. 2003. Environmental quality and carrying capacity for aquaculture in Mulroy Bay Co. Donegal. *Marine Environment and Health Series* No. 9

Tetra Tech, 1980. *Methodology for evaluation of multiple power plant cooling system effect, Volume V*. Methodology Application to Prototype – Cayuga Lake. Tetra Tech, Inc., Lafayette, California. For Electric Power Research institute. Report EPRI EA-III.

Thomann, R.V., and Kirkpatrick, J.J., 1982. *Calibration and validation of a mathematical model of the eutrophication of the Potomac estuary*, Prepared for the Department of Environmental Services, Government of the District of Colombia.

Waite, R.P., 1989. The Nutritional Biology of *Perna canaliculus* With Special Reference to Intensive Mariculture Systems. Unpublished PhD thesis, University of Canterbury, Christchurch, New Zealand.

## APPENDIX 1: 3DDLIFE FUNCTIONS

**PHYTOPLANKTON**

The overall mass balance for phytoplankton is modelled as

$$\frac{dP}{dt} = \text{production - death - settling - grazing} \qquad \textbf{(1)}$$

Phytoplankton growth ($\mu$) is a function of light $f$(I), temperature $f$(T), and dissolved nutrients $f$(N,P)

$$\text{production} = \mu_P = \mu_{P\max} f(T) \times f(I) f(N,P) \bullet P \qquad \textbf{(2)}$$

Where $\mu_{\text{pmax}}$ is the maximal growth rate of the phytoplankton at a reference temperature (20$^o$C) and under an optimal light and nutrient environment (time$^{-1}$), $f(T)$, $f(I)$, and $f(N,P)$ are temperature, light, and nutrient limitation functions respectively.

**Temperature Function**

The temperature function $f(T)$ represents the effects of ambient temperature variations on the maximal algal growth. Elevated temperatures result in more rapid growth of phytoplankton. The temperature function must be consistent with the reference temperature used in $\mu_{\text{pmax}}$. The most widely used function in the literature is based on the Arrhenuis equation (Eppley, 1972)

$$f(T) = \theta^{(T-20^o C)} \qquad \textbf{(3)}$$

Where $\theta$ is the temperature adjustment coefficient (with mean of 1.066, Eppley, 1972), and T is the ambient water temperature ($^o$C).

**Light Function**

Separate growth limiting functions are usually computed for light and each limiting nutrient (Bowie *et al.*, 1985). Each limitation factor varies between 0 and 1, with 0 resulting in the factor inhibiting all growth, while a value of 1 results in no limitation due to the factor under consideration.

Two factors must be taken into consideration with the light function, 1) the effect of light levels on phytoplankton growth and 2) the attenuation of light with depth (with respect to water clarity, etc.).

Light attenuation with depth is modelled with Beers law

$$I_{(z)} = I_o e^{-K_L z} \quad \textbf{(4)}$$

Where $I_{(z)}$ is the solar radiation (W $m^{-2}$) at depth $z$ (m), $I_o$ is the incoming solar radiation at the water surface (W $m^{-2}$) and $K_L$ is the extinction co-efficient ($m^{-1}$) of light within the water column. This equation is integrated over depth and the mean value for the depth layer in question is used. The surface light intensity used is only that within the visible range as other wavelengths are absorbed within the first meter, this typically corresponds to 50% of the total solar radiation used in heat budget calculations (Bowie *et al.*, 1985).

To model the effect of light levels on phytoplankton growth, Steele's (1965) photosynthesis-irradiance function is widely used (e.g. Chapelle *et al.* 2000). The function incorporates the photo-inhibition effect at higher than optimal light levels.

$$f(I) = \frac{I_z}{I_{opt}} e^{\left(1-\frac{I_z}{I_{opt}}\right)} \quad \textbf{(5)}$$

Where $I_{opt}$ is the optimal light intensity (W $m^{-2}$) (prior to photo-inhibition). (Figure 2.)

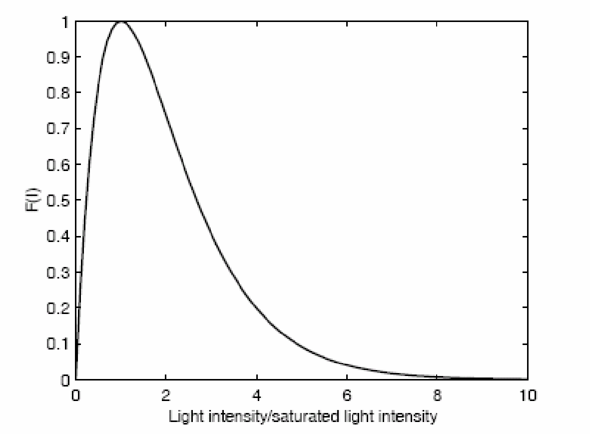


**Figure 0.1 – Value of the light function used in the calculation of the production of phytoplankton and light intensity:optimal light intensity ratio.**

***Nutrient Function***

Dissolved nutrients control phytoplankton growth. In general the limiting nutrient is nitrogen, however this can be phosphorus or sometimes silica in the case of diatoms. The limiting nutrient is generally the deficient nutrient with respect to the Redfield ratio. The function $f$(N) is the nutrient limited growth rate reduction factor (dimensionless). 3DDLIFE uses the Michaelis-Menten function to describe nutrient limitation with respect to phytoplankton

$$f(N) = \frac{N}{k_N + N} \qquad \textbf{(6)}$$

Where N is the nutrient concentration ($mass.volume^{-1}$) and $k_N$ is the half saturation constant ($mass.volume^{-1}$) i.e. the concentration of the nutrient at which the rate of growth is half the maximum (Figure 3.3). A separate function $f$(N) is determined for both nitrogen ($NOx + NH_4$) and phosphorus.

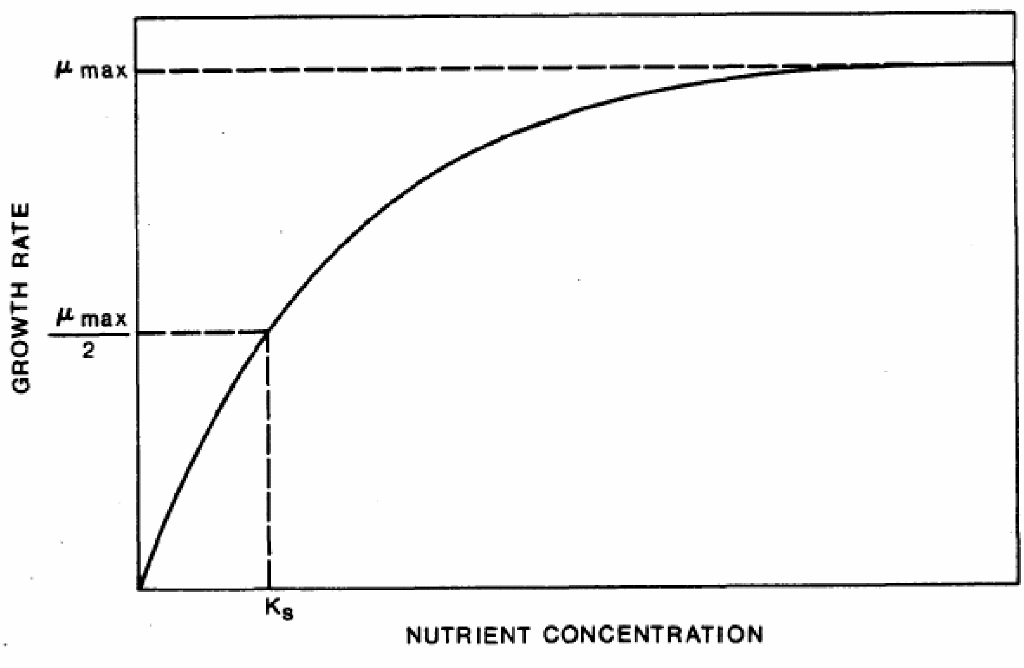


**Figure 0.2 – Algal growth rate and nutrient concentration modelled with the Michaelis-Menten function.**

A harmonic mean formulation is used to combine the effects of both nitrogen limitation and phosphorus limitation, while the light function is assumed to be multiplicative,

$$f(I)f(N,P) = f(I) \times \frac{2}{\frac{1}{f(N)} + \frac{1}{f(P)}} \quad \textbf{(7)}$$

The fixed stoichiometry scheme of the model assumes that algal growth is limited by external concentrations of nutrients, and that internal ratios of these nutrients are fixed (to the redfield molar ratio of 106:16:1 for C:N:P). This contrasts to variable stoichiometry models which allow the luxury uptake of nutrients by phytoplankton and results in growth being limited by the internal pools of nitrogen and phosphorus.

***Nutrient Uptake by Photosynteshisers***

The nature of the fixed stoichiometry scheme of the model means that nutrient uptake by photosynthesisers is directly related to their growth rate, as a result of the fixed composition of the cells.

$$\text{uptake}_N = \mu_P \gamma \bullet P \quad \textbf{(8)}$$

Where $\text{uptake}_N$ is the uptake rate of the nutrient (mass_nutrient.mass_algae$^{-1}$time$^{-1}$), $\mu_P$ is the growth rate of phytoplankton (time$^{-1}$) and $\gamma$ is the constant internal nutrient concentration (ratio of nutrient:biomass) (mass_nutrient.biomass_algae$^{-1}$). Thus the change in water column nutrient concentrations is

$$\frac{dN}{dt} = N_{ex\_in} - \gamma \mu_P \bullet P \quad \textbf{(9)}$$

Where N is the nutrient concentration in the water column and $N_{ex\_in}$ is the exogenous nett rate of supply of nutrients.

***Ammonia Preference***

Since algae use two forms of nitrogen (nitrate and ammonia) during uptake and growth, an ammonia preference factor must be incorporated into the model in order to account for the fact that phytoplankton will preferentially uptake ammonia over nitrate. Thus the uptake equations for nitrogen become

$$\text{uptake}_{NH_3} = \beta_{NH3} \mu_P \gamma \bullet P, \quad \text{and} \quad \textbf{(10)}$$

$$\text{uptake}_{NO_x} = (1 - \beta_{NH3}) \mu_P \gamma \bullet P \quad \textbf{(11)}$$

Where $\beta_{NH3}$ is the ammonia preference factor, which can range form 1 (all the phytoplankton nitrogen requirements are gained from ammonia) to 0 (all the phytoplankton nitrogen requirements are gained from nitrate). The value of the ammonia preference factor is a function of the relative concentrations of ammonia and nitrate in the water column,

$$\beta_{NH3} = \frac{NH_3}{NH_3 + NO_x} \quad \textbf{(12)}$$

***Phytoplankton Death (Non-predatory)***

Non-predatory phytoplankton mortality is modelled as a function of temperature (e.g. Eppley, 1972; Chapelle *et al.*, 2000).

$$d_P = \mu_{deathP\max} f(T) \bullet P \quad \textbf{(13)}$$

Where $d_P$ is the phytoplankton mortality rate (day$^{-1}$), and $\mu_{deathPmax}$ is the maximum mortality rate at the reference temperature (day$^{-1}$). The temperature function here has an identical form to that of equation 3.

***Phytoplankton Settling***

Phytoplankton settling is modelled by incorporating a typical settling velocity for the entire phytoplankton population. The phytoplankton settling velocity is input specifically as a model constant. The effects of temperature on the density and viscosity of the water are incorporated through the use of a temperature function (equation 14)

$$s = V_s \times \frac{157.5}{0.069T^2 - 5.3T + 177.6} \quad \textbf{(14)} \quad \textbf{(Tetra Tech, 1980)}$$

Where s is the temperature specific settling velocity (m.s$^{-1}$), $V_s$ is the reference settling velocity at 20$^o$C (m.s$^{-1}$), and T is the water temperature in $^o$C.

***Grazing on Phytoplankton by Zooplankton***

The grazing on phytoplankton is back-calculated from the zooplankton growth rates, a common method of determining the rate at which zooplankton feed on phytoplankton.

$$G_Z = \frac{g_Z}{E} \bullet Z \quad \textbf{(15)}$$

Where $G_Z$ is the grazing on phytoplankton by zooplankton (gP/gZ.day), $g_Z$ is the zooplankton growth rate (day$^{-1}$), and $E$ is the assimilation efficiency of the zooplankton. See zooplankton section for controls on zooplankton growth.

**ZOOPLANKTON**

The overall mass balance for zooplankton is modelled as

$$\frac{dZ}{dt} = \text{ growth - (respiration and excretion) - death} \qquad \textbf{(16)}$$

***Zooplankton Growth***

Zooplankton growth ($g_Z$) is a function of temperature, food concentrations and the zooplankton assimilation efficiency.

$$g_Z = g_{Zref} f(T) f(P) \qquad \textbf{(17)}$$

Where $g_{Zref}$ is the reference zooplankton growth rate at 20$^{o}$C (day$^{-1}$), *f(T)* is a temperature function of similar form to equation 3 (though with differing constants), and *f(P)* is an ivlev-type limitation factor based on food availability

$$f(P) = 1 - e^{(-K(P-P_T))}$$
$$K = -\frac{\ln(0.5)}{K_Z} \qquad \textbf{(18)}$$

Where $K_Z$ is the half saturation constant for zooplankton feeding and growth (g/m$^3$), $P$ is the zooplankton food density (assumed to be phytoplankton) (g/m$^3$), and $P_T$ is the threshold food density, below which no feeding occurs (g/m$^3$).

***Zooplankton respiration***

Zooplankton respiration is modelled as a function of both temperature and the activity of the zooplankton

$$r_Z = r_{Zref} f(T) \frac{g_Z}{E} \qquad \textbf{(19)}$$

Where $r_Z$ is the respiration of the zooplankton, $r_{Zref}$ is the reference zooplankton respiration at 20C, *f(T)* is a temperature function, the same as in equation 17, $g_Z$ is the zooplankton growth rate from equation 16.

***Zooplankton non-predatory death***

Zooplankton mortality is modelled as a function of temperature,

$$d_z = d_{zref} f(T) \quad \textbf{(20)}$$

Where $d_{zref}$ is the reference zooplankton mortality at 20°C (day$^{-1}$) and $f(T)$ is a temperature function as in equation 17.

***Zooplankton excretion***

Zooplankton excretion is modelled as the difference between grazing, production, and respiration.

$$Z_{excr} = \max(\frac{g_z}{E} - g_z - r_z - d_z, 0) \quad \textbf{(21)}$$

These excretion products enter the detritus and organic matter pools as detailed in the appropriate mass balance equations.

**DETRITUS**

Both detrital nitrogen and phosphorus are simulated in the model, with the equations essentially being the same, though differing constants and reference values may be used for the mineralization of species etc.

$$\frac{dDETRITUS}{dt} = \text{generation - sedimentation - mineralization} \quad \textbf{(22)}$$

***Detritus Generation***

Detritus is added to the water column through dead phytoplankton, dead zooplankton, and the excretion of material by zooplankton

$$generation = (1 - P_{\min imm}) d_P RR_{Px} + d_Z RR_{Zx} + (1 - Z_{excr \min imm}) Z_{excr} RR_{Zx} \quad \textbf{(23)}$$

Where $P_{minimm}$ is the fraction of dead phytoplankton which is mineralised immediately, $RR_P$ is the Redfield ratio (mass wise) of the nutrient under consideration in the phytoplankton, $RR_Z$ is the Redfield ratio (mass wise) of the nutrient under consideration in zooplankton, $Z_{excrminimm}$ is the fraction of excreted zooplankton material which is mineralised immediately.

***Detritus mineralization (M)***

The mineralization of detrital nitrogen and phosphorus into their inorganic forms is simulated by the model as a function of temperature and the oxygen environment. The mineralization of detritus not only regenerates the inorganic nutrients but also causes oxygen consumption.

$$\mathrm{M} = M_{ref} f(T) f(DO) \tag{24}$$

Where $M_{ref}$ is the reference mineralization rate at 20°C ($day^{-1}$), *f(T)* is a temperature function of similar form to equation 17 to represent an increase in the rate of mineralization at elevated temperatures, and *f(DO)* is a dissolved oxygen function to indicate a reduction in mineralization at low oxygen concentrations,

$$f(DO) = \frac{DO^2}{DO^2 + MDO} \tag{25}$$

Where DO is the dissolved oxygen concentration of the water body ($g/m^3$) and MDO is the oxygen concentration indicating depleted rates of mineralization due to low oxygen levels ($g/m^3$).

***Detritus Sedimentation***

Detrital particles fall down through the water column at a velocity defined by the user.

**INORGANIC NUTRIENTS**

***Ammonia***

Ammonia is generated through the mineralization of detrital nitrogen and is consumed by phytoplankton photosynthesising and by nitrification of ammonia to nitrate.

$$\frac{dNH_3}{dt} = M.DN + Z_{excr} Z_{excr\,\min imm} RR_{Zn} + P_{\min imm} d_P RR_{Pn} - uptake_{NH_3} - N_R NH_3 \tag{26}$$

Where $N_R$ is the nitrification rate ($day^{-1}$) which varies with temperature according to the equation

$$N_R = N_{Rref} \theta_N^{(T-20)} \tag{27}$$

Where $N_{Rref}$ is the reference nitrification rate at 20°C, and $\theta_N$ is the nitrification temperature coefficient.

***Nitrate***

Oxidised nitrogen is generated by the nitrification of ammonia and removed by the uptake by photosynthesisers.

$$\frac{dNO_x}{dt} = N_R NH_3 - uptake_{NO_x} \quad \textbf{(28)}$$

***Inorganic Phosphorus***

Inorganic phosphorus is generated through the mineralization of detrital phosphorus and is consumed by phytoplankton photosynthesising.

$$\frac{dPO_4}{dt} = M.DP + Z_{excr} Z_{excr\,\min imm} RR_{Zp} + P_{\min imm} d_P RR_{Pp} - uptake_{PO_4} \quad \textbf{(29)}$$

**DISSOLVED OXYGEN**

Dissolved oxygen is modelled as the difference between both production and re-aeration and consumption,

$$\frac{dDO}{dt} = production + reaeration - consumption \quad \textbf{(30)}$$

Reaeration is only valid however at the water-air interface.

***Production***

Oxygen is produced by photosyntheising phytoplankton. A specific amount of oxygen is produced per gram of biomass

$$O_P = \mu_P V_o \quad \textbf{(31)}$$

Where $V_o$ is the oxygen to biomass ratio at production ($gO_2$/g.algae).

***Consumption***

Oxygen is consumed by the respiration of zooplankton, the mineralization of detrital nitrogen and phosphorus, the mineralization of dead phytoplankton and zooplankton, and by the nitrification of ammonia to nitrate.

$$O_C = r_z.V_o + M.V_o + P_{\min imm} d_p + Z_{excr \min imm} Z_{excr} + 4.5714 N_R \qquad \textbf{(32)}$$

[for every gram of $NH_3$ nitrified to $NO_x$ , 4.5714 grams of oxygen is consumed according to the equation NH4 + 2O2 > NO3 + H2O + H]

***Reaeration***

The reaeration at the water – air interface is determined from the oxygen saturation concentration and the reaeration rate.

$$DO_{SAT} = 14.652 - 0.0841S + T(0.00256S - 0.41022 + T\{0.007991 - 0.0000374S - 0.000077774T\})$$

**(33)**

$$DO_{\mathrm{Rear}} = (DO_{SAT} - DO)\left[\frac{(0.728W^{0.5} - 0.317W + 0.0372W^2)}{h} + 3.93\left(\frac{V^{0.5}}{h^{1.5}}\right)\right]$$

**(34) (Thomann and Fitzaptrick, 1982)**

Where W is the surface wind speed ($m.s^{-1}$), h is the depth of the surface layer (m) and V is the velocity of the water surface ($m.s^{-1}$).

**MUSSEL FEEDING DYNAMICS**

Mussel feeding dynamics are incorporated into the model at all levels.

Mussel clearance (filtration) rates are defined by the user. The mussels then filter the water at this rate and extract particles (phytoplankton, zooplankton, detritus) from the water dependant on both the concentration of the particle within the water body and the mussel filtering efficacy for the specific particle.

The various mass balance equations (phytoplankton, zooplankton, detritus) are modified with the addition of another term:

$$-M_{CL}.f(T).M.E_M.P \qquad \textbf{(35)}$$

where $M_{CL}$ is the clearance rate of the mussels ($m^3.g.day^{-1}$), M is the mussel biomass ($g/m^3$), $E_M$ is the filtration efficacy for the particles being filtered (in this case Phytoplankton) (n.u.), and P is the concentration of the particles being filtered ($g/m^3$).

In addition to filtering particles from the water column, the mussels excrete ammonia and consume oxygen. These processes are modelled by inserting an additional term into the ammonia mass balance and dissolve oxygen mass balance equations as follows:

Ammonia:

$$+M_{excr} f(T) M \quad \textbf{(36)}$$

**and**

Dissolved Oxygen

$$-M_{resp} M \quad \textbf{(37)}$$

Where $M_{excr}$ is the excretion rate of $NH_3$ by the mussels ($gNH_3.day^{-1}.g^{-1}$), and $M_{resp}$ is the respiration rate of the mussels ($gO_2.day^{-1}.g^{-1}$).